



Journal of Applied and Computational Mechanics



Review Paper

A Brief Review on the Asymptotic Methods for the Periodic Behaviour of Microelectromechanical Systems

Naveed Anjum¹, Ji-Huan He^{2,3}, Chun-Hui He⁴, Alina Ashiq⁵

¹ Department of Mathematics, Government College University, Faisalabad, Pakistan

² National Engineering Laboratory for Modern Silk, College of Textile and Engineering, Soochow University, Suzhou, China

³ School of Mathematics and Information Science, Henan Polytechnic University, Jiaozuo, China

⁴ School of Civil Engineering, Xi'an University of Architecture and Technology, Xi'an, China

⁵ Department of Physics, Government College University, Faisalabad, Pakistan

Received December 07 2021; Revised March 09 2022; Accepted for publication March 10 2022.

Corresponding author: J.H. He (hejihuan@suda.edu.cn)

© 2022 Published by Shahid Chamran University of Ahvaz

Abstract. Microelectromechanical systems (MEMS) is a very vast field and has been identified as lots of potential in tiny instruments. Because of their unique and exciting properties such as small sizes, low power consumption, reliability, and their capability of batch fabrications, their role in the production of microstructures has gained much importance for researchers and industries. The following study includes an overview of current asymptotic approaches and novel innovations which are applicable not only to weakly nonlinear equations but also to highly nonlinear equations derived from MEMS models. Moreover, the approximate analytical solutions obtained by these asymptotic approaches are valid across the whole solution domain. Various limitations of traditional perturbation method and variational iteration method are discussed and different modified versions of perturbation approaches and variational theory are provided to overcome these existing flaws. Two-scale idea for MEMS technology is also described. Some examples are given to elucidate the effectiveness and convenience of these methodologies.

Keywords: Asymptotic methods, Nonlinear oscillators, Microelectromechanical systems, Amplitude-frequency relationship, Periodic solutions, Two-scale vibration.

1. Introduction

Microelectromechanical systems (MEMS) is a very vast field and has been identified as lots of potential in tiny instruments [1-4]. Because of their unique and exciting properties such as small sizes, low power consumption, reliability, and their capability of batch fabrications, their role in the production of microstructures has gained much importance for researchers and industries [5-6]. Pull-in instability and periodic behaviour are two key phenomenon in MEMS dynamics and differential equations can be well described these nonlinear aspects. Therefore, it is vital to have a keen familiarity with recently developed methods for exploring the solutions of the differential equations.

Principally, MEMS models are nonlinear, and solving such mathematical models analytically is challenging in most scenarios. There are numerous nonlinear equations in the study of MEMS research that do not have analytical solutions [7-10]. Many analytical and numerical techniques have been studied due to the limitations of current precise solutions. As a result, these nonlinear equations must be solved using different approaches. Over the last few decades, many academics have been working on various analytical approaches for addressing nonlinear oscillation of MEMS. The classical approaches for oscillatory theory have several flaws for the case of these microstructures [10]. They are ineffective for solving highly nonlinear equations, so numerous new approaches have emerged in the open literature to compensate. Moreover, there are several books have appeared on the subject of mathematical methods in MEMS problems during the past decade [10-13].

The purpose of this article is to provide an overview of recent researches on approximate analytical techniques for nonlinear vibrations of MEMS. In the last few years, applications of these approaches have surfaced in open literature. There are too many published articles to include them all, but refs [14, 15] may be useful in filling in the gaps in the current overview. Some comparisons have been made between the results produced by those techniques and numerical methods to demonstrate the efficiency and accuracy of the methods, and they are valid for the entire domain. Some of the ideas were originally presented in this review paper, and the majority of the listed references were published within the previous three years, highlighting the most recent research frontiers. The basic notion of each technique is provided in this review, followed by some examples that are shown and discussed to demonstrate the use of these methods.



2. MEMS Models

MEMS are fascinating new technologies with astonishing mechanical, electrical and optical properties. They consist of fixed and movable parts. Upon supplying an actuation force, the moveable part is bent toward the fixed part and a periodic motion is produced in the system. Therefore, we can say that MEMS come with spring or spring-like structures, for example, beams. Two widely used structures for MEMS technology are clamped-clamped microbeam model [16-20] and lumped-parameter model [7-8, 21-22].

2.1 Clamped-clamped microbeam based MEMS

Suppose a clamped-clamped MEMS with dimensions L , b , h and ρ depict length, width, thickness and density of the microbeam, respectively, shown in Figure 1. The deflection of microbeam is based on Newton's Law and can be modelled mathematically by employing Euler-Bernoulli beam theory [23-24] as

$$EI \frac{\partial^4 W}{\partial z^4} + \rho S \frac{\partial^2 W}{\partial \tau^2} - \left[\tilde{N} + \frac{ES}{2L} \int_0^L \left(\frac{\partial W}{\partial z} \right)^2 dz \right] \frac{\partial^2 W}{\partial z^2} - F(z, \tau) = 0 \tag{1}$$

where z denotes the location at time τ and $W(z, \tau)$ symbolizes the deflection of microbeam. Additionally, E indicates the Young's modulus, $S = bh$ and $I = bh^3/12$ are the cross-sectional area and moment of inertia about Y axis respectively. \tilde{N} and $F(z, \tau)$ correspondingly shown the axial load and actuating force between microbeam and its substrate. If we suppose the van der Waals force for sensing purpose between the nanobeam and substrate [25]:

$$F(z, \tau) = \frac{G_h b}{6\pi(d - W)^3} \tag{2}$$

where G_k indicates the Hamaker constant [25]. The boundary conditions will be

$$W(0, \tau) = W(L, \tau) = 0, \quad \left. \frac{\partial W}{\partial z} \right|_{(0, \tau)} = \left. \frac{\partial W}{\partial z} \right|_{(L, \tau)} = 0 \tag{3}$$

For simplicity, the nondimensional variables can be chosen as

$$\eta = \frac{z}{L}, \quad w = \frac{W}{d}, \quad t = \frac{\tau}{\tilde{T}} \tag{4}$$

where

$$\tilde{T} = \sqrt{\frac{\rho h b L^4}{EI}} \tag{5}$$

Eq. (1) will get the form as:

$$\frac{\partial^4 w}{\partial \eta^4} + \frac{\partial^2 w}{\partial t^2} - \left[N + \alpha \int_0^1 \left(\frac{\partial w}{\partial \eta} \right)^2 d\eta \right] \frac{\partial^2 w}{\partial \eta^2} - \frac{\lambda}{(1 - w)^3} = 0 \tag{6}$$

where nondimensional parameters N , α and λ represent axial load, aspect ratio and van der Waals force and can be defined as:

$$N = \frac{\tilde{N}L^2}{EI}, \quad \alpha = 6 \left(\frac{d}{h} \right)^2, \quad \lambda = \frac{12G_h}{Eh^3} \left(\frac{L}{d} \right)^4 \tag{7}$$

Also the nondimensional form of boundary conditions can be expresses as

$$w(0, t) = w(1, t) = 0, \quad \left. \frac{\partial w}{\partial \eta} \right|_{(0, t)} = \left. \frac{\partial w}{\partial \eta} \right|_{(1, t)} = 0 \tag{8}$$

The governing equation developed here represents a general form for the oscillatory behaviour of the nanobeam. To find out the nonlinear ordinary differential equation of the system, we apply the Galerkin method. Hence it is possible to write the deflection function $w(\eta, t)$ as the combination of two functions

$$w(\eta, t) = \xi(\eta)z(t) \tag{9}$$

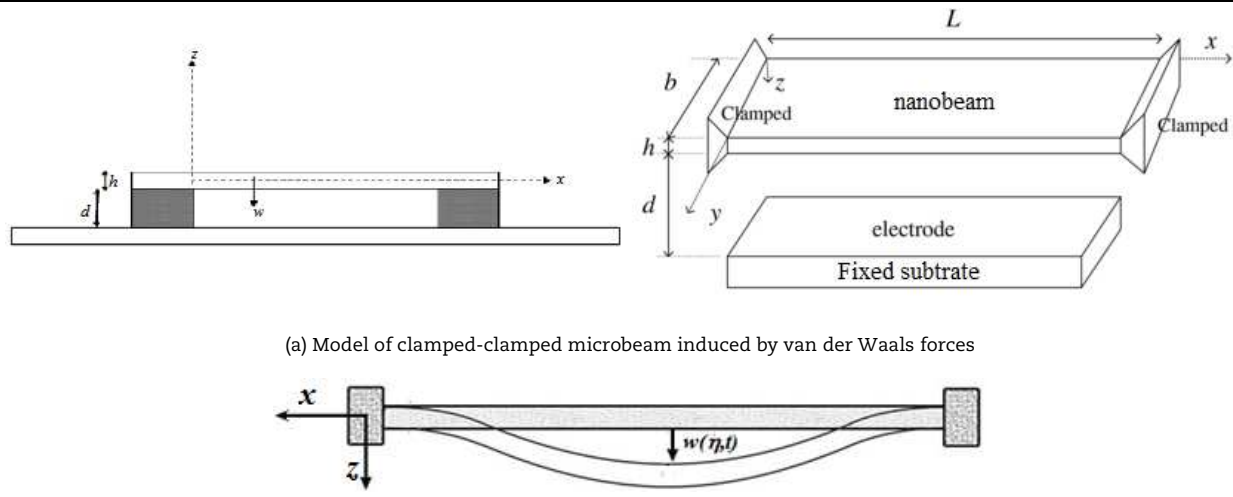
where $z(t)$ is the function of time and $\xi(\eta)$ is the trail function as

$$\xi(\eta) = 16\eta^2(1 - \eta)^2 \tag{10}$$

For the governing equation, we substitute Eq. (9) in Eq. (6), multiplied by $\xi(\eta)(1 - w)^3$ and then integrate over dimensionless domain results

$$\int_0^1 \xi(1 - \xi z)^3 z \xi'''' d\eta + \int_0^1 \xi^2(1 - \xi z)^3 z'' d\eta - \int_0^1 \xi(1 - \xi z)^3 \left[N + \alpha \int_0^1 \left(\frac{\partial w}{\partial \eta} \right)^2 d\eta \right] z \xi'' d\eta - \int_0^1 \lambda \xi d\eta = 0 \tag{11}$$





(a) Model of clamped-clamped microbeam induced by van der Waals forces

(b) Change of deflection in microbeam

Fig. 1. Clamped-clamped microbeam based MEMS

where prime (•′) represents the partial differentiation w.r.t coordinate variable η and over dot (•̇) represents the differentiation w.r.t time variable t . Eq. (11) can be rewritten as

$$(h_0 + h_1z + h_2z^2 + h_3z^3)\ddot{z} + h_4 + h_5z + h_6z^2 + h_7z^3 + h_8z^4 + h_9z^5 + h_{10}z^6 = 0 \tag{12}$$

where the coefficients h_j ($j=0,1,\dots,10$) can be found in Appendix A. Eq. (12) is a nonlinear ordinary differential equation of second order under the following initial conditions

$$z(0) = G, \quad z'(0) = 0 \tag{13}$$

If actuation is based on electrostatic force [25] given by

$$F(x, \tau) = \frac{b\nu^2\epsilon_\nu}{2} \left[\frac{1}{(d - W)^2} - \frac{1}{(d + W)^2} \right] \tag{14}$$

where ν denotes the applied voltage, ϵ_ν is dielectric constant with value usually 8.85PFm^{-1} and d is the initial gap between substrate and beam. Then by applying the similar procedure as applied for the case of van der Waals force, we have the equation for MEMS oscillator actuated electrically expressed by

$$(c_0 + c_1z^2 + c_2z^4)\ddot{z} + c_3z + c_4z^3 + c_5z^5 + c_6z^7 = 0 \tag{15}$$

where the coefficients h_j ($j=0,1,\dots,10$) can be found in Appendix B.

2.2 Lumped-parameter MEMS

Our system is based on the magnetic actuation [26-28] and the force F between two straight wires can be expressed by

$$F = \frac{\mu_0 I_1 I_2}{2\pi R} \tag{16}$$

where $\mu_0 = 4\pi \times 10^{-7} \text{NA}^{-2}$ is the constant, I_1 and I_2 are the currents through the wires separated by distance R . We suppose the deflection of a current-carrying wire of length L and mass m shown in Figure 2. The motion of the moveable part is restrained by linear elastic springs. The dynamic differential equation describing the motion of the wire as a point mass can be derived using Eq. (1) and theory of modelling of elastic Euler beam as

$$m\ddot{u} + k\bar{u} - \frac{\mu_0 I_1 I_2 L}{2\pi(B - \bar{u})} = 0 \tag{17}$$

where $F = \mu_0 I_1 I_2 / 2\pi R$ is the restoring force of spring and $F = \mu_0 I_1 I_2 / 2\pi R$ is the force of attraction between the conductors due to the magnetic fields produced by I_1 and I_2 . The model in dimensionless form is

$$\ddot{z} + z - \frac{\kappa}{1 - z} = 0 \tag{18a}$$

where

$$z = \frac{\bar{u}}{B}, \quad t = \bar{t}\omega_0, \quad u = \frac{\bar{u}}{B}, \quad \kappa = \frac{\mu_0 I_1 I_2 L}{2\pi kB} \tag{18b}$$

We propose the initial conditions zero

$$z(0) = 0, \quad \dot{z}(0) = 0 \tag{19}$$



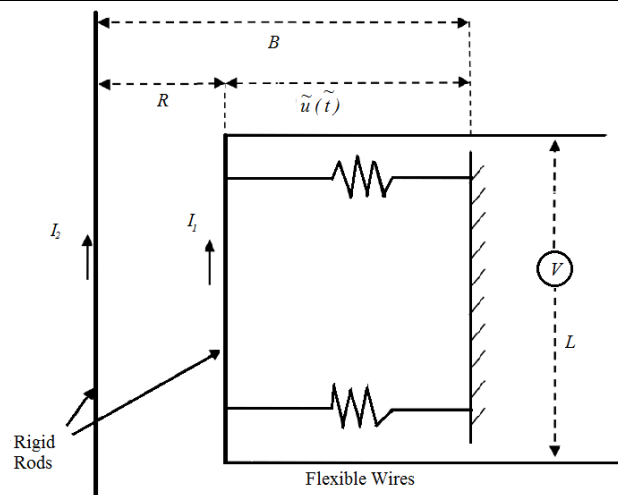


Fig. 2. MEMS with a current carrying wire

We also prescribe the current in both wires are unidirectional i.e., $\kappa \geq 0$. We can describe Eq. (18) as a system of first order differential equations

$$\begin{aligned} \dot{z} &= v \\ \dot{v} &= z - \frac{\kappa}{1-z} \end{aligned} \tag{20}$$

and the conditions will become

$$z(0) = 0, \quad v(0) = 0 \tag{21}$$

3. Variational Iteration Method

Nonlinear phenomena are important in applied mechanics and physics. We can help writers understand the given process better by solving nonlinear equations. However, it is not easy for us to find an exact or at least an analytic solution to these problems. There has been significant progress in the numerical analysis and obtaining exact solutions of nonlinear equations in recent decades. There are spectrum of methods for solving nonlinear differential equations. The variational iteration method (VIM) was first proposed by He [29] and is used to obtain approximate analytical solutions for nonlinear problems. In most situations, just one iteration is required in VIM to achieve high accuracy of the answer, and no linearization, discretization, or substantial computing labor is required. The VIM can be used to solve linear and nonlinear differential equations, both exactly and approximately [30-35]. We looked at three instances to demonstrate how the VIM may be used.

3.1 Basic idea of VIM

The goal of VIM is to create the appropriate correction functional with a Lagrange multiplier that is optimally predicted by theory of variations. Consider the following differential equation in a broad sense to grasp the basic idea of VIM

$$Lz + Nz = h(t) \tag{22}$$

where L and N are respectively the linear and the nonlinear operators, and $h(t)$ is inhomogeneous term. According to standard VIM, the correction iteration for Eq. (22) can be depicted as

$$z_{m+1}(t) = z_m(t) + \int_0^t \lambda(\psi) [Lz_m(\psi) + Nz_m(\psi) + h(\psi)] d\psi, \quad m = 0, 1, 2, \dots \tag{23}$$

where λ is the Lagrange multiplier could be a fixed or variable parameter of t identified optimally via variational theory and by using the restricted variation z_m which means $\delta z_m = 0$. z_m represents the k th approximate function, whereas any selective function can be objected as zeroth-approximation z_m for VIM, and based on this initial guess, the solution is structured as

$$z(t) = \lim_{m \rightarrow \infty} z_m(t) \tag{24}$$

3.2 Laplace transform based VIM

Laplace transformation is the well-known integral transform accessible to all students and can solve linear ordinary, partial, and integral equations in the time domain. To solve nonlinear problems quickly, many researchers paired this transformation with the VIM [36-39]. Now we'll look at a different method for determining the Lagrange multiplier. The coupling of the VIM with the Laplace transform has two primary goals in this section. Find the amplitude-frequency relationship of a nonlinear oscillatory system by first identifying the Lagrange multiplier.

3.2.1 Analysis of the Laplace-based VIM

Let a general oscillatory system can be represented as:

$$\ddot{z}(t) + h(z) = 0 \tag{25}$$



$$z(0) = G, \quad \dot{z}(0) = 0 \tag{26}$$

We can express Eq. (25) as

$$\ddot{z} + \Omega^2 z + g(z) = 0 \tag{27}$$

where $g(z) = h(z) - \Omega^2 z$. According to standard VIM [29], we can construct the correction functional for Eq. (27) as

$$z_{m+1}(t) = z_m(t) + \int_0^t \lambda(\psi) [\ddot{z}_m(\psi) + \Omega^2 z_m(\psi) + \tilde{g}_m(\psi)] d\psi, \quad m = 0, 1, 2, \dots \tag{28}$$

where λ is the Lagrange multiplier, z_m represents the k th approximate solution, and \tilde{g}_m is a restricted variation, i.e., $\delta \tilde{g}_m = 0$. Here we discussed an alternative way to identify the Lagrange multiplier which is the backbone of the VIM. Generally we choose the multiplier as

$$\lambda = \bar{\lambda}(t - \psi)$$

The integral of Eq. (28) is basically the convolution; thus we can employ Laplace transformation easily. Utilizing the properties of the Laplace transform, the correction function will be changed in the following way

$$L[z_{m+1}(t)] = L[z_m(t)] + L\left[\int_0^t \lambda(t - \psi) [\ddot{z}_m(\psi) + \Omega^2 z_m(\psi) + \tilde{g}_m(\psi)] d\psi\right], \quad m = 0, 1, 2, \dots \tag{29}$$

Thus

$$\begin{aligned} L[z_{m+1}(t)] &= L[z_m(t)] + L[\lambda(t) * (\ddot{z}_m(t) + \Omega^2 z_m(t) + \tilde{g}_m(t))] \\ &= L[z_m(t)] + L[\lambda(t)] L[(\ddot{z}_m(t) + \Omega^2 z_m(t) + \tilde{g}_m(t))] \end{aligned} \tag{30}$$

$$L[z_{m+1}(t)] = L[z_m(t)] + L[\lambda(t)] L[(s^2 + \Omega^2)L[z_m(t)] - sz_m(0) - \dot{z}_m(0) + L[\tilde{g}_m(z)]]$$

To find λ optimally, we firstly take variation with respect to z_n and then by employing the stationary condition as

$$\frac{\delta}{\delta z_n} L[z_{m+1}(t)] = \frac{\delta}{\delta z_n} L[z_m(t)] + \frac{\delta}{\delta z_n} L[\lambda(t)] [(s^2 + \Omega^2)L[z_m(t)] - sz_m(0) - \dot{z}_m(0) + L[\tilde{g}_m(z)]] \tag{31}$$

$$L[\delta z_{m+1}] = L[\delta z_m] + L[\lambda] (s^2 + \Omega^2) L[\delta z_m(t)]$$

$$L[\lambda] = -\frac{1}{(s^2 + \Omega^2)} \tag{32}$$

or

$$\lambda(t) = -\frac{1}{\Omega} \sin \Omega t \tag{33}$$

Using Eq. (29), the formula gets the form

$$L[z_{m+1}(t)] = L[z_m(t)] - \frac{1}{\Omega} L\left[\int_0^t \sin \Omega(t - \psi) [\ddot{z}_m(\psi) + \omega^2 z_m(\psi) + \tilde{g}_m(\psi)] d\psi\right]$$

or

$$L[z_{m+1}(t)] = L[z_m(t)] - \frac{1}{\Omega} L[\sin \Omega t] L[\ddot{z}_m(\psi) + \Omega^2 z_m(\psi) + \tilde{g}_m(\psi)] \tag{34}$$

By applying the properties of Laplace transformation, we can achieve the higher-order solution by using the formula in Eq. (34).

3.2.2 Example

Now we apply LVIM to find the approximate solution of Eq. (12). For this we can depict Eq. (12) in the following manner

$$(1 + d_1 z + d_2 z^2 + d_3 z^3) \ddot{z} + d_4 + d_5 z + d_6 z^2 + d_7 z^3 + d_8 z^4 + d_9 z^5 + d_{10} z^6 = 0 \tag{35}$$

where $d_j = h_j / h_0$ for $j = 1, 2, \dots, 10$. Let us rewrite Eq. (35) as

$$\ddot{z} + \Omega^2 z + g(z) = 0 \tag{36}$$

where $g(z) = (d_1 z + d_2 z^2 + d_3 z^3) \ddot{z} + d_4 + (d_5 - \Omega^2) z + d_6 z^2 + d_7 z^3 + d_8 z^4 + d_9 z^5 + d_{10} z^6$. The iterative formula for Eq. (36) using LVIM can be written as

$$L[z_{m+1}(t)] = L[z_m] - \frac{1}{\omega} L[\sin \omega t] L[(1 + d_1 z_m + d_2 z_m^2 + d_3 z_m^3) \ddot{z}_m + d_4 + d_5 z_m + d_6 z_m^2 + d_7 z_m^3 + d_8 z_m^4 + d_9 z_m^5 + d_{10} z_m^6] \tag{37}$$



Assuming the initial solution

$$z_0(t) = G \cos \Omega t \tag{38}$$

After simple calculations, we have

$$L[z_1(t)] = L[G \cos \Omega t] - \frac{1}{\Omega} L[\sin \Omega t] L[\Theta_0 + \Theta_1 \cos \Omega t + \Theta_2 \cos 2\Omega t + \Theta_3 \cos 3\Omega t + \Theta_4 \cos 4\Omega t + \Theta_5 \cos 5\Omega t + \Theta_6 \cos 6\Omega t] \tag{39}$$

where the expression of coefficients $\Theta_0, \Theta_1, \dots, \Theta_6$ can be depicted in Appendix B.

The following formula helps us to solve Eq. (39)

$$L^{-1}(L[\sin \Omega t] L[\cos \kappa \Omega t]) = \begin{cases} \frac{1}{2} t \sin \Omega t, & \kappa = 1 \\ \frac{\cos \Omega t - \cos \kappa \Omega t}{\Omega(\kappa^2 - 1)}, & \kappa \neq 1 \end{cases} \tag{40}$$

$$z_1 = G \cos \Omega t + \frac{\Theta_0}{\Omega^2} (\cos \Omega t - 1) - \frac{\Theta_1}{2\Omega} t \sin \Omega t - \frac{\Theta_2}{3\Omega^2} (\cos \Omega t - \cos 2\Omega t) - \frac{\Theta_3}{8\Omega^2} (\cos \Omega t - \cos 3\Omega t) - \frac{\Theta_4}{15\Omega^2} (\cos \Omega t - \cos 4\Omega t) - \frac{\Theta_5}{24\Omega^2} (\cos \Omega t - \cos 5\Omega t) - \frac{\Theta_6}{35\Omega^2} (\cos \Omega t - \cos 6\Omega t) \tag{41}$$

No secular-term [40-42] in the next step requires that coefficient of $t \sin \Omega t$ equal to zero, thus

$$\frac{\Theta_1}{2\Omega} = 0 \tag{42a}$$

or

$$-G\Omega^2 \left(1 + \frac{3d_2 G^2}{4} \right) + Gd_5 + \frac{3d_7 G^3}{4} + \frac{5d_9 G^5}{8} = 0 \tag{42b}$$

yields

$$\Omega = \sqrt{\frac{8d_5 + 6d_7 G^2 + 5d_9 G^4}{8 + 6d_2 G^2}} \tag{43}$$

and thus the approximate analytic solution of the Eq. (12) is

$$z_{VIM} = a_0 + (a_1 + G) \cos \Omega t + a_2 \cos 2\Omega t + a_3 \cos 3\Omega t + a_4 \cos 4\Omega t + a_5 \cos 5\Omega t + a_6 \cos 6\Omega t \tag{44}$$

where

$$a_0 = -\frac{\Theta_0}{\Omega^2}, \quad a_1 = \frac{1}{\Omega^2} \left(\Theta_0 - \frac{\Theta_2}{3} - \frac{\Theta_3}{8} - \frac{\Theta_4}{15} - \frac{\Theta_5}{24} - \frac{\Theta_6}{35} \right), \quad a_2 = \frac{\Theta_2}{3\Omega^2}, \tag{45}$$

$$a_3 = \frac{\Theta_3}{8\Omega^2}, \quad a_4 = \frac{\Theta_4}{15\Omega^2}, \quad a_5 = \frac{\Theta_5}{24\Omega^2}, \quad a_6 = \frac{\Theta_6}{35\Omega^2}$$

The validity of the proposed method is discussed through a comparison of the results obtained by LVIM with those got numerically using RK4 and a comparison of the results achieved by LVIM with those gained using SRHBM [43]. Figure 3 illustrates the effectiveness of the proposed method. It represents the deflection obtained analytically from numerical solution for the motion of nanobeams induced by van der Waals attraction. We have also shown the variation of error for the above-mentioned system in the corresponding bottom panels.

3.3 LVIM for zero initial conditions

Several MEMS like Eq. (18) come with zero initial conditions. Therefore, it is necessary to be familiar with the strategy to solve MEMS models with zero initial conditions. LVIM has the tendency to do this and equally applicable for the said case. The following subsection focuses on using LVIM, which was explained in Section 3.2.1, to examine the dynamic behaviour of the nonlinear MEMS models with zero initial conditions [44].

3.3.1 Basic Methodology

Consider the oscillatory system as

$$\frac{d^2 z(t)}{dt^2} + f(z) = 0 \tag{46}$$

$$z(0) = 0, \quad \left. \frac{dz}{dt} \right|_{t=0} = 0 \tag{47}$$

We can rewrite the iterative formula from Eq. (34)

$$L[z_{m+1}(t)] = L[z_m(t)] - \frac{1}{\Omega} L \left[\int_0^t \sin \Omega(t - \psi) \left[\frac{d^2 z_m(\psi)}{d\psi^2} + \Omega^2 z_m(\psi) + \tilde{g}_m(z) \right] d\psi \right] \tag{48}$$



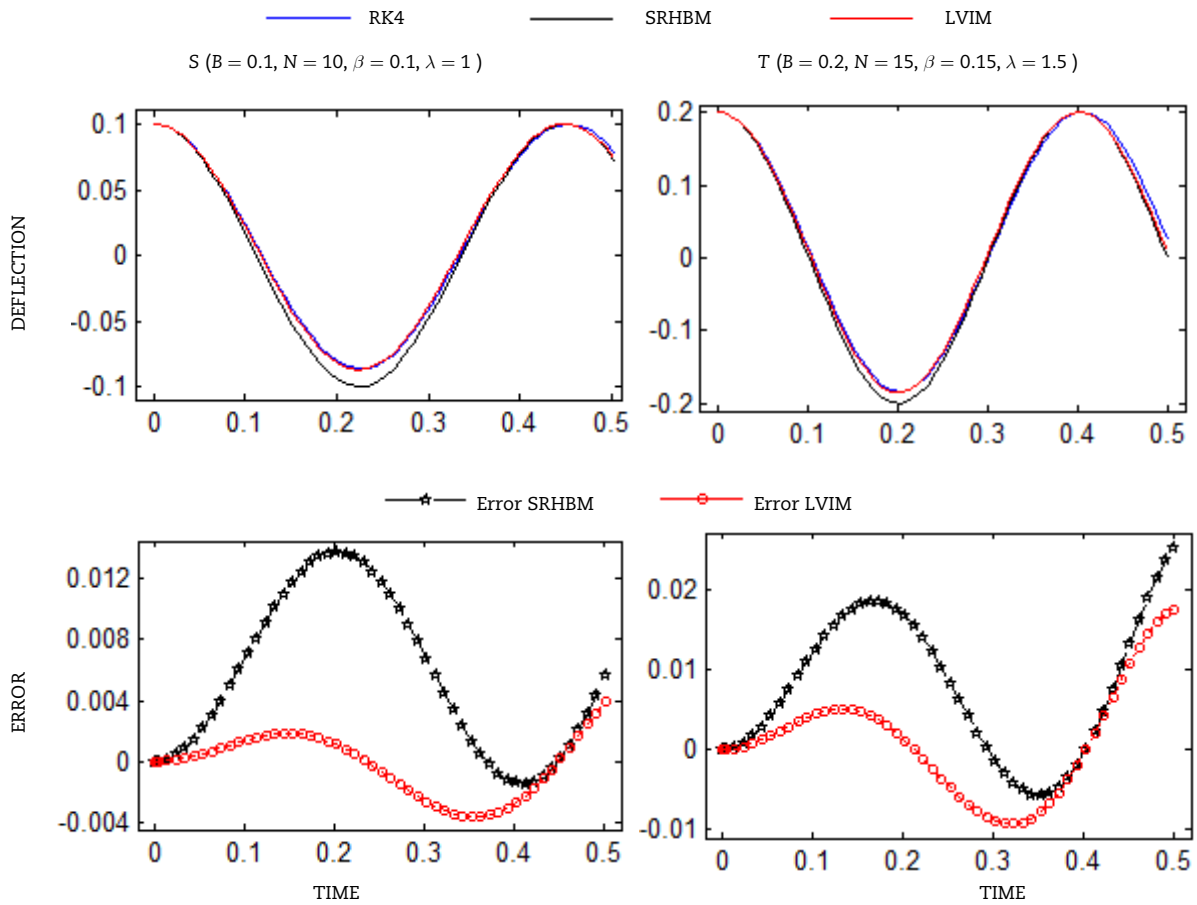


Fig. 3. Comparison of deflection and error in deflection between LVIM and SRHBM with RK4

Consider the following integration by parts

$$\int \sin \Omega(t - \psi) \frac{d^2 z_m(\psi)}{d\psi^2} d\psi = \sin \Omega(t - \psi) \frac{dz_m(\psi)}{d\psi} + \Omega \int \cos \Omega(t - \psi) \frac{dz_m(\psi)}{d\psi} d\psi$$

$$\int \sin \Omega(t - \psi) z_m(\psi) d\psi = \frac{1}{\Omega} \cos \Omega(t - \psi) z_m(\psi) - \frac{1}{\Omega} \int \cos \Omega(t - \psi) \frac{dz_m(\psi)}{d\psi} d\psi$$
(49)

The following integral can be obtained using Eq. (49), as follows:

$$\int_0^t \sin \Omega(t - \psi) \left[\frac{d^2 z_m(\psi)}{d\psi^2} + \Omega^2 z_m(\psi) \right] d\psi = -\sin \Omega t \frac{dz_m(t)}{dt} \Big|_{t=0} + \Omega z_m(t) - \Omega z_m(0) \cos \Omega t$$
(50)

Eq. (48), after employing Eq. (50), has the form

$$L[u_{m+1}(t)] = -\frac{1}{\Omega} L \left[-\sin \Omega t \frac{dz_m(t)}{dt} \Big|_{t=0} - \Omega z_m(0) \cos \Omega t + \int_0^t \sin \Omega(t - \psi) [\tilde{g}_m(z)] d\psi \right]$$
(51)

After employing zero initial conditions, the correction functional reduced further as

$$L[z_{m+1}(t)] = -\frac{1}{\Omega} L \left[\int_0^t \sin \Omega(t - \psi) [\tilde{g}_m(z)] d\psi \right]$$
(52a)

or, we have

$$L[z_{m+1}(t)] = -\frac{1}{\Omega} L[\sin \Omega t] L[g(z_m(t))]$$
(52b)

3.3.2 Example

Now we employ LVIM for the nonlinear Eq. (18) subject to the zero initial conditions. From the truncated Taylor series we can discretize the rational term as

$$(1 + z)^{-1} = 1 - z + z^2 - z^3 + z^4 - \dots \quad -1 < z < 1$$
(53)



Thus Eq. (18) will achieve the following form

$$\frac{d^2z}{dt^2} + z - \kappa(1 + z + z^2 + z^3) = 0 \tag{54}$$

Eq. (54) can also be rewrite in the following way

$$\frac{d^2z}{dt^2} + \Omega^2z + g(z) = 0 \tag{55}$$

where

$$g(z) = z(1 - \kappa - \Omega^2) - \kappa(1 + z^2 + z^3) \tag{56}$$

The iteration formula for Eq. (54) can be attained by using Eq. (52)

$$L[z_{m+1}(t)] = -\frac{1}{\Omega}L[\sin \Omega t]L[z_m(1 - \kappa - \Omega^2) - \kappa(1 + z_m^2 + z_m^3)] \tag{57}$$

Due to the zero initial conditions, let $z_0(t) = 0$. Thus, Eq. (57) will become

$$L[z_1(t)] = \frac{1}{\Omega}L[\sin \Omega t]L[\kappa]$$

After utilizing the properties of Laplace transformation, we have

$$z_1(t) = \frac{\kappa}{\Omega^2}(1 - \cos \Omega t) \tag{58}$$

For higher-order solution, substitute Eq. (58) into Eq. (57)

$$L[z_2(t)] = -\frac{1}{\Omega}L[\sin \Omega t]L\left[\frac{\kappa}{\Omega^2}(1 - \cos \Omega t)(1 - \kappa - \Omega^2) - \kappa\left[1 + \left(\frac{\kappa}{\Omega^2}(1 - \cos \Omega t)\right)^2 + \left(\frac{\kappa}{\Omega^2}(1 - \cos \Omega t)\right)^3\right]\right]$$

Simple calculations yield

$$L[z_2(t)] = -\frac{1}{\Omega}L[\sin \Omega t]L\left[\left(\frac{\kappa}{\Omega^2} - 2\kappa - \frac{\kappa^2}{\Omega^2} - \frac{\kappa^3}{\Omega^4} - \frac{\kappa^4}{\Omega^6}\right) + \frac{\kappa^4}{\Omega^6}\cos^3 \Omega t - \left(\frac{\kappa^3}{\Omega^4} + \frac{3\kappa^4}{\Omega^6}\right)\cos^2 \Omega t + \left(-\frac{\kappa}{\Omega^2} + \kappa + \frac{\kappa^2}{\Omega^2} + \frac{2\kappa^3}{\Omega^4} + \frac{15\kappa^4}{4\Omega^6}\right)\cos \Omega t\right] \tag{59}$$

$$L[z_2(t)] = -\frac{1}{\Omega}L[\sin \Omega t]L\left[\left(\frac{\kappa}{\Omega^2} - 2\kappa - \frac{\kappa^2}{\Omega^2} - \frac{3\kappa^3}{2\Omega^4} - \frac{5\kappa^4}{2\Omega^6}\right) + \frac{\kappa^4}{4\Omega^6}\cos 3\Omega t - \left(\frac{\kappa^3}{2\Omega^4} + \frac{3\kappa^4}{2\Omega^6}\right)\cos 2\Omega t + \left(-\frac{\kappa}{\Omega^2} + \kappa + \frac{\kappa^2}{\Omega^2} + \frac{2\kappa^3}{\Omega^4} + \frac{15\kappa^4}{4\Omega^6}\right)\cos \Omega t\right]$$

Using formula in Eq. (40) helps to solve above Eq. (59) and we obtain the following result

$$z_2(t) = -\frac{1}{\Omega}\left[\left(\frac{\kappa}{\Omega^2} - 2\kappa - \frac{\kappa^2}{\Omega^2} - \frac{3\kappa^3}{2\Omega^4} - \frac{5\kappa^4}{2\Omega^6}\right)\frac{1}{\Omega}(1 - \cos \Omega t) + \frac{\kappa^4}{4\Omega^6}\frac{1}{8\Omega}(\cos \Omega t - \cos 3\Omega t) - \left(\frac{\kappa^3}{2\Omega^4} + \frac{3\kappa^4}{2\Omega^6}\right)\frac{1}{3\Omega}(\cos \Omega t - \cos 2\Omega t) + \left(-\frac{\kappa}{\Omega^2} + \kappa + \frac{\kappa^2}{\Omega^2} + \frac{2\kappa^3}{\Omega^4} + \frac{15\kappa^4}{4\Omega^6}\right)\frac{1}{2}t \sin \Omega t\right] \tag{60}$$

For periodic solution, secular term must be zero. i.e.,

$$4\Omega^6 + (4\kappa - 4)\Omega^4 + 8\kappa^2\Omega^2 + 15\kappa^3 = 0 \tag{61}$$

The approximate second-order solution is found as

$$z_2(t) = -\frac{1}{\Omega}\left[\left(\frac{\kappa}{\Omega^2} - 2\kappa - \frac{\kappa^2}{\Omega^2} - \frac{3\kappa^3}{2\Omega^4} - \frac{5\kappa^4}{2\Omega^6}\right)\frac{1}{\Omega}(1 - \cos \Omega t) + \frac{\kappa^4}{4\Omega^6}\frac{1}{8\Omega}(\cos \Omega t - \cos 3\Omega t) - \left(\frac{\kappa^3}{2\Omega^4} + \frac{3\kappa^4}{2\Omega^6}\right)\frac{1}{3\Omega}(\cos \Omega t - \cos 2\Omega t)\right] \tag{62}$$

$$z_2(t) = \frac{1}{96\Omega^8}(-195\kappa^4 - 128\kappa^3\Omega^2 + 96\kappa\Omega^4 - 96\kappa^2\Omega^4 - 192\kappa\Omega^6)\cos \Omega t + \frac{\kappa^4}{32\Omega^8}\cos 3\Omega t - \frac{1}{6\Omega^8}(3\kappa^4 + \kappa^3\Omega^2)\cos 2\Omega t + \frac{1}{2\Omega^8}(5\kappa^4 + 3\kappa^3\Omega^2 - 2\kappa\Omega^4 + 2\kappa^2\Omega^4 + 4\kappa\Omega^6)$$

Eq. (62) depicts the second-order approximate solution of MEMS switch model. The beauty of this approach is not only provide approximate analytic solution but also gives the threshold value of dynamic pull-in. When we solve Eq. (61) for angular frequency by any method for solving cubic equation, we have



$$\Omega = \sqrt{\left(Q + \sqrt{Q^2 + P^3}\right)^{1/3} + \left(Q - \sqrt{Q^2 + P^3}\right)^{1/3}} - \frac{\kappa - 1}{3} \tag{63}$$

where

$$P = -\frac{1}{9} + \frac{2\kappa}{9} + \frac{5\kappa^2}{9}, \quad Q = \frac{1}{27} - \frac{\kappa}{9} - \frac{2\kappa^2}{9} - \frac{341\kappa^3}{216}$$

The discriminant of Eq. (61) yields the pull-in threshold value that is $\kappa = 0.20498371\dots$ with the percentage error is less than 1%. This threshold value can differentiate between the periodic solution and the pull-in solution.

4. Homotopy Perturbation Method

Scientists and engineers have been committed to the use of the homotopy perturbation approach in nonlinear issues until recently, because this method continually deforms a simple problem that is easy to solve into the complex problem under investigation. The homotopy perturbation method (HPM) was proposed by He in 1999 [45]. The following papers [46-48] provide a basic overview and interpretation of the approach. HPM is capable of solving a wide range of nonlinear problems [49-55], with approximations quickly convergent to correct solutions. For the both weakly and highly nonlinear problems, this approach is the most efficient and convenient.

4.1 Basic idea of HPM

The homotopy perturbation technique (HPM) [51] is a combination of the perturbation method and the homotopy method that eliminates the shortcomings of classic perturbation methods. Considering a nonlinear differential equation to show the basic concept of HPM [52] as:

$$D(z) - g(v) = 0, \quad v \in \Psi \tag{64}$$

with boundary condition

$$G\left(z, \frac{\partial z}{\partial \eta}\right) = 0, \quad v \in \Lambda \tag{65}$$

where D is a general differential operator, G is a boundary operator, $g(v)$ is a known analytical function and Λ is the boundary of the domain Ψ . The differential operator D can be split into two parts: linear L and nonlinear N . Therefore, Eq. (64) can be written as:

$$L(z) + N(z) - g(v) = 0 \tag{66}$$

We generate the following homotopy using the HPM

$$H(\xi, q) = (1 - q)[L(\xi) - L(\xi_0)] + q[D(\xi) - g(v)] = 0, \quad q \in [0, 1] \tag{67}$$

where q is the perturbation parameter and ξ_0 is a starting guess of Eq. (64) which fulfills the given conditions generally. Clearly, from Eq. (67)

$$H(\xi, 0) = L(\xi) - L(\xi_0) = 0 \tag{68}$$

$$H(\xi, 1) = A(\xi) - g(v) = 0 \tag{69}$$

The embedding parameter q is used as an expanding parameter in HPM [51] and the key hypothesis is that Eq. (67)'s solution may be expressed as a power series in q :

$$\xi = \xi_0 + q\xi_1 + q^2\xi_2 + q^3\xi_3 + q^4\xi_4 + \dots \tag{70}$$

Setting $q = 1$ gives the approximate analytic solution of Eq. (67) as

$$u = \lim_{q \rightarrow 1} \xi = \xi_0 + \xi_1 + \xi_2 + \xi_3 + \xi_4 + \dots \tag{71}$$

The series in Eq. (70) may converge in the whole solution domain as q tends to unit.

4.2 Laplace transform based HPM

All students are familiar with the Laplace transform, although it is only useful for linear problems. The HPM and the Laplace transform were initially combined by Gondal and Khan [56], and the technique is now known as the He-Laplace method [57-60]. The most notable aspect of this method is that it just takes one iteration to get great precision in the solution. The small number of perturbation terms is enough for obtaining a reasonably accurate solution to a problem. We combine this approach with the Laplace transformation to obtain the solution to the oscillation problem using only couple of perturbation terms [58]. Another superiority of this approach over the traditional HPM [45] is that we discretize the nonlinear term with the help of He's polynomials [61], and the solution process becomes easy.

4.2.1 Analysis of the method

Consider the following equation for a general nonlinear oscillator:

$$\ddot{z}(t) + f(z) = h(t) \tag{72}$$



with initial conditions expressed in Eq. (26). We can depict Eq. (72) as

$$\ddot{z} + \omega^2 z + g(z) = h(t) \tag{73}$$

where $g(z) = f(z) - \Omega^2 z$. One can rewrite Eq. (73) as

$$\ddot{z} + \Omega^2 z + Rg(z) + Ng(z) = h(t) \tag{74}$$

where $Rg(z)$ and $Ng(z)$ are respectively the linear and the nonlinear part of $g(z)$. Ω is the frequency of the oscillation and $h(t)$ is an inhomogeneous term. Apply the Laplace transformation to each side of the Eq. (74), we have

$$s^2 z(s) - Gs + \Omega^2 z(s) + L[Rg(z) + Ng(z)] = L[h(t)] \tag{75}$$

$$z(s) = \frac{Gs}{s^2 + \Omega^2} - \frac{1}{s^2 + \Omega^2} L[Rg(z) + Ng(z)]$$

Inverse Laplace transform of Eq. (75) yields

$$z(t) = G \cos \Omega t - L^{-1} \left[\frac{1}{s^2 + \Omega^2} L[Rg(z) + Ng(z)] \right] + L^{-1} \left[\frac{1}{s^2 + \Omega^2} L[h(t)] \right] \tag{76}$$

According to standard HPM [45] the solution z can be expanded

$$z(t) = \sum_{m=0}^{\infty} p^m z_m \tag{77a}$$

and Eq. (76) has the form

$$\sum_{m=0}^{\infty} p^m z_m = G \cos \Omega t - p \left(L^{-1} \left[\frac{1}{s^2 + \Omega^2} L[Rg(z) + Ng(z)] \right] - L^{-1} \left[\frac{1}{s^2 + \Omega^2} L[h(t)] \right] \right) \tag{77b}$$

where $p \in [0,1]$ is an embedding parameter. Also, the nonlinear term $Ng(z)$ can be written as

$$Ng(z) = \sum_{m=0}^{\infty} p^m H_m(z) \tag{78}$$

where $H_m(z)$ are the He's polynomials [61] and can be generated by the recursive formula

$$H_m(z_0, z_1, \dots, z_m) = \frac{1}{m!} \frac{\partial^m}{\partial p^m} \left[Ng \left(\sum_{i=0}^{\infty} p^i z_i(t) \right) \right]_{p=0}, \quad m = 0, 1, 2, \dots \tag{79}$$

The solution can be stated as by inserting Eq. (78) for Eq. (77)

$$\sum_{m=0}^{\infty} p^m z_m = G \cos \Omega t - p \left(L^{-1} \left[\frac{1}{s^2 + \Omega^2} \{ L[Rg(z)] + L[H_m] \} \right] - L^{-1} \left[\frac{1}{s^2 + \Omega^2} L[h(t)] \right] \right) \tag{80}$$

When the coefficients of like powers of p are compared, we have

$$p^0 : \quad z_0 = G \cos \Omega t \tag{81}$$

$$p^1 : \quad z_1 = -L^{-1} \left[\frac{1}{s^2 + \Omega^2} \{ L[Rg(z_0)] + L[H_0] \} \right] + L^{-1} \left[\frac{1}{s^2 + \Omega^2} L[h(t)] \right] \tag{82}$$

$$p^2 : \quad z_2 = -L^{-1} \left[\frac{1}{s^2 + \Omega^2} \{ L[Rg(z_1)] + L[H_1] \} \right] + L^{-1} \left[\frac{1}{s^2 + \Omega^2} L[h(t)] \right] \tag{83}$$

⋮

As $p \rightarrow 1$, we can write the solution approximately is

$$z(t) = \lim_{p \rightarrow 1} \sum_{n=0}^{\infty} p^n z_n(t) = z_0(t) + z_1(t) + z_2(t) + \dots \tag{84}$$

Although we can use z_0, z_1, z_2, \dots to find the approximate solution of the oscillatory system but for simplicity, we use only Eq. (101) and Eq. (102). In this scenario, Eq. (102) will express in its simple form as

$$z_1 = -L^{-1} \left[\frac{1}{s^2 + \Omega^2} L[g(z_0)] \right] + L^{-1} \left[\frac{1}{s^2 + \Omega^2} L[h(t)] \right] \tag{85}$$

From the above Eq. (85), we can obtain a relationship between Ω and G by means of secular term and then use this relation in Eq. (84) to get a fairly accurate solution of Eq. (72). From Eq. (84), it can be observed that the approximate solution $z(t)$ is not depending on p (expanding parameter) or some other perturbative factor.



4.2.2 Example

To apply HPM on the objective model Eq. (12), consider Eq. (14)

$$\ddot{z} + \Omega^2 z + g(z) = 0 \tag{86}$$

where

$$g(z) = (d_1 z + d_2 z^2 + d_3 z^3) \dot{z} + d_4 + (d_5 - \Omega^2) z + d_6 z^2 + d_7 z^3 + d_8 z^4 + d_9 z^5 + d_{10} z^6 \tag{87}$$

Employing the Laplace transformation to both side of Eq. (86), we yield

$$s^2 z(s) - Gs + \Omega^2 z(s) + L[(d_1 z + d_2 z^2 + d_3 z^3) \dot{z} + d_4 + (d_5 - \Omega^2) z + d_6 z^2 + d_7 z^3 + d_8 z^4 + d_9 z^5 + d_{10} z^6] = 0$$

$$z(s) = \frac{Gs}{s^2 + \Omega^2} - \frac{1}{s^2 + \Omega^2} L[(d_1 z + d_2 z^2 + d_3 z^3) \dot{z} + d_4 + (d_5 - \Omega^2) z + d_6 z^2 + d_7 z^3 + d_8 z^4 + d_9 z^5 + d_{10} z^6]$$

Using the inverse Laplace transformation on both side of the above equation, we have

$$z(t) = G \cos \Omega t - L^{-1} \left[\frac{1}{s^2 + \Omega^2} L[(d_1 z + d_2 z^2 + d_3 z^3) \dot{z} + d_4 + (d_5 - \Omega^2) z + d_6 z^2 + d_7 z^3 + d_8 z^4 + d_9 z^5 + d_{10} z^6] \right] \tag{88}$$

According to the HPM [45], the solution can be expressed

$$z(t) = \sum_{m=0}^{\infty} p^m z_m$$

and Eq. (88) has the form

$$\sum_{m=0}^{\infty} p^m z_m = G \cos \Omega t - p \left(L^{-1} \left[\frac{1}{s^2 + \Omega^2} L \left[(d_5 - \Omega^2) \sum_{m=0}^{\infty} p^m z_m + \sum_{m=0}^{\infty} p^m H_m \right] \right] \right) \tag{89}$$

where H_m denotes the He's polynomials [61] to discretize the nonlinear terms. When the coefficients of like powers of p are compared, we yield

$$p^0 : \quad z_0 = G \cos \Omega t \tag{90}$$

$$p^1 : \quad z_1 = -L^{-1} \left[\frac{1}{s^2 + \Omega^2} L[(d_5 - \Omega^2) z_0 + H_0] \right]$$

$$= -L^{-1} \left[\frac{1}{s^2 + \Omega^2} L[g(z_0)] \right] \tag{91}$$

$$= -L^{-1} \left[\frac{1}{s^2 + \Omega^2} L[\Theta_0 + \Theta_1 \cos \Omega t + \Theta_2 \cos 2\Omega t + \Theta_3 \cos 3\Omega t + \Theta_4 \cos 4\Omega t + \Theta_5 \cos 5\Omega t + \Theta_6 \cos 6\Omega t] \right]$$

where the coefficients $\Theta_i (i = 0, 1, \dots, 6)$ are the same as that expressed in equations A1-A7. Upon solving Eq. (91) with Laplace and inverse Laplace operators, we have

$$p^1 : \quad z_1 = \frac{\Theta_0}{\Omega^2} (\cos \Omega t - 1) - \frac{\Theta_1}{2\Omega} t \sin \Omega t - \frac{\Theta_2}{3\Omega^2} (\cos \Omega t - \cos 2\Omega t) - \frac{\Theta_3}{8\Omega^2} (\cos \Omega t - \cos 3\Omega t) - \frac{\Theta_4}{15\Omega^2} (\cos \Omega t - \cos 4\Omega t)$$

$$- \frac{\Theta_5}{24\Omega^2} (\cos \Omega t - \cos 5\Omega t) - \frac{\Theta_6}{35\Omega^2} (\cos \Omega t - \cos 6\Omega t) \tag{92}$$

No secular-term [40-42] demands that coefficient of $t \sin \Omega t$ must equals to zero, thus

$$\frac{\Theta_1}{2\Omega} = 0$$

$$-G\Omega^2 \left(1 + \frac{3d_2 G^2}{4} \right) + Gd_5 + \frac{3d_7 G^3}{4} + \frac{5d_9 G^5}{8} = 0$$

As a result, the following is the outcome

$$\Omega = \sqrt{\frac{8d_5 + 6d_7 G^2 + 5d_9 G^4}{8 + 6d_2 G^2}} \tag{93}$$

and thus

$$p^1 : \quad z_1 = a_0 + a_1 \cos \Omega t + a_2 \cos 2\Omega t + a_3 \cos 3\Omega t + a_4 \cos 4\Omega t + a_5 \cos 5\Omega t + a_6 \cos 6\Omega t \tag{94}$$

where

$$a_0 = -\frac{\Theta_0}{\Omega^2}, a_1 = \frac{1}{\Omega^2} \left(\Theta_0 - \frac{\Theta_2}{3} - \frac{\Theta_3}{8} - \frac{\Theta_4}{15} - \frac{\Theta_5}{24} - \frac{\Theta_6}{35} \right), a_2 = \frac{\Theta_2}{3\Omega^2}, a_3 = \frac{\Theta_3}{8\Omega^2}, a_4 = \frac{\Theta_4}{15\Omega^2}, a_5 = \frac{\Theta_5}{24\Omega^2}, a_6 = \frac{\Theta_6}{35\Omega^2}$$



As a result, the approximate first-order analytic solution of Eq. (12) can be written as

$$z_{\text{HPLTM}} = a_0 + (a_1 + G)\cos\Omega t + a_2 \cos 2\Omega t + a_3 \cos 3\Omega t + a_4 \cos 4\Omega t + a_5 \cos 5\Omega t + a_6 \cos 6\Omega t \quad (95)$$

4.3 Higher-order HPM

Analytic approaches have become a helpful tool for discovering hidden phenomena in diverse nonlinear issues as a result of the rapid development of nonlinear sciences. The HPM is the most widely utilized technology, having been proposed in the late 1990s [45-48] and having progressed to a mature state. However, due to the advancement of other analytical techniques, the procedure still has room for improvement. This section will describe the enhanced perturbation approach, which was proposed in 2018[62], as the most recent advancement in the conventional perturbation method. This improvement is particularly well suited to oscillatory situations involving forced terms. This latest modifications in HPM used in various applications including packing system technology [63-65].

4.3.1 Analysis of the method

To understand the basic idea of the recent modification, consider the forced linear oscillator

$$z'' + \Omega^2 z = \cos\Omega t \quad (96)$$

In operator form, Eq. (96) can be written as

$$(D^2 + \Omega^2)z = \cos\Omega t \quad (97)$$

where $D = d/dt$ is an operator. The annihilator operator $D^2 + \Omega^2$ is used in the enhanced perturbation method. Therefore, Eq. (97) will get the form:

$$(D^2 + \Omega^2)(D^2 + \Omega^2)z = z'''' + 2\Omega^2 z'' + \Omega^4 z = 0 \quad (98)$$

This method can be used to tackle a wide range of nonlinear systems. It works best in nonlinear models with a forced term, although it can also be used in applications without forced term. Eq. (98) becomes a higher-order equation after some acceptable substitutions, and it may be expressed in linear and nonlinear operator form as:

$$Lz + Nz = 0 \quad (99)$$

where L and N are supposed to be linear and nonlinear operators, respectively. We employ the enhanced perturbation method with parameter expansion technology to solve the oscillatory equation. Therefore, the solution and the coefficient of linear term (say clt) can be depicted as:

$$z = z_0 + pz_1 + p^2 z_2 + \dots \quad (100)$$

$$clt = \Omega^4 + a_1 p + a_2 p^2 + \dots \quad (101)$$

where constants Ω^4 and a_i can be identified by means of no secular term and p is an embedding parameter with value $[0,1]$. Finally, the approximate analytic solution of Eq. (99) can be obtained in series form

$$z = z_0 + z_1 + z_2 + \dots \quad (102)$$

The series in Eq. (102) may converge in the whole solution domain as p tends to unit.

4.3.2 Example

To apply higher-order HPM on Eq. (15), we can represent it in the following way

$$(1 + b_1 z^2 + b_2 z^4)\ddot{z} + b_3 \dot{z} + b_4 z^3 + b_5 z^5 + b_6 z^7 = 0 \quad (103)$$

where $b_j = c_j / c_0$ for $j = 0, 1, 2, \dots, 6$. We express Eq. (103) in an operator form as

$$[D^2(1 + b_1 z + b_2 z^3) + b_3 + b_4 z^2 + b_5 z^4 + b_6 z^6]z = 0 \quad (104)$$

According to the technique described in above section, we apply the operator $D^2 + 1$ to Eq. (104)

$$(D^2 + 1)[D^2(1 + b_1 z + b_2 z^3) + b_3 + b_4 z^2 + b_5 z^4 + b_6 z^6]z = 0 \quad (105)$$

The higher-order differential equation of Eq. (104) can be expressed as

$$z'''' - b_2^2 z - b_3 b_4 z^3 - b_3 b_5 \lambda z^5 - b_3 b_6 z^7 - b_1 b_3 \lambda z^2 z'' - b_2 b_3 \lambda z^4 z'' + b_4 (6zz''^2 + 3z^2 z'') + b_5 (20z^3 z''^2 + 5z^4 z'') + b_6 (42z^5 z''^2 + 7z^6 z'') \\ + b_1 (2z''^2 z'' + 2zz''^2 + 4zz' z''') + b_2 (12z^2 z''^2 z'' + 4z^3 z''^2 + 8z^3 z' z''') + z^4 z'''' = 0 \quad (106)$$

The linear part becomes now

$$z'''' - b_3^2 z = 0 \quad (107)$$

which denotes a linear oscillator. For Eq. (106), the homotopy equation can express as



$$z'''' - b_3^2 z + p[-b_3 b_4 z^3 - b_3 b_5 \lambda z^5 - b_3 b_6 z^7 - b_1 b_3 \lambda z^2 z'' - b_2 b_3 \lambda z^4 z'' + b_4(6zz'^2 + 3z^2 z'') + b_5(20z^3 z'^2 + 5z^4 z'') + b_6(42z^5 z'^2 + 7z^6 z'')] + b_1(2z'^2 z'' + 2zz''^2 + 4zz' z''') + b_2(12z^2 z'^2 z'' + 4z^3 z''^2 + 8z^3 z' z'' + z^4 z''') = 0 \tag{108}$$

where the solution and the linear term coefficient can be expanded as

$$z = z_0 + pz_1 + p^2 z_2 + \dots \tag{109}$$

$$b_3^2 = \Omega^4 + p\Omega_1 + p^2\Omega_2 + \dots \tag{110}$$

where Ω^4 and Ω_i are constants and can be found with the help of no secular term. Applying Eqs. (109) and (110) into Eq. (108) and continuing as that by the standard perturbation method, we have

$$z_0'''' - \Omega^4 z_0 = 0 \quad z_0(0) = A, \quad z_0'(0) = 0 \tag{111}$$

$$z_1'''' - \Omega^4 z_1 - \Omega_1 z_0 - b_3 b_4 z_0^3 - b_3 b_5 z_0^5 - b_3 b_6 z_0^7 - b_1 b_3 z_0^2 z_0'' - b_2 b_3 z_0^4 z_0'' + b_4(6z_0 z_0'^2 + 3z_0^2 z_0'') + b_5(20z_0^3 z_0'^2 + 5z_0^4 z_0'') + b_6(42z_0^5 z_0'^2 + 7z_0^6 z_0'') + b_1(2z_0'^2 z_0'' + 4z_0 z_0' z_0''') + z_0^2 z_0'''' + 2z_0 z_0''^2 + b_2(12z_0^2 z_0'^2 z_0'' + 4z_0^3 z_0''^2 + 8z_0^3 z_0' z_0'' + z_0^4 z_0''') = 0 \tag{112}$$

We can use Eq. (13) to get a rough estimate of the initial solution

$$z_0 = A \cos \Omega t \tag{113}$$

After using the initial solution, Eq. (102) will have the form

$$z_1'''' - \Omega^4 z_1 - G\Omega_1 \cos \Omega t - b_3 b_4 [G^3 \cos^3 \Omega t] - b_3 b_5 [G^5 \cos^5 \Omega t] - b_3 b_6 [G^7 \cos^7 \Omega t] - b_1 b_3 [-G^3 \Omega^2 \cos^3 \Omega t] - b_2 b_3 [-G^5 \Omega^2 \cos^5 \Omega t] + b_4 [6G^3 \Omega^2 \cos \Omega t - 9G^3 \Omega^2 \cos^3 \Omega t] + b_5 [20G^5 \Omega^2 \cos^3 \Omega t - 25G^5 \Omega^2 \cos^5 \Omega t] + b_6 [42G^7 \Omega^2 \cos^5 \Omega t - 49G^7 \Omega^2 \cos^7 \Omega t] + b_1 [-6G^3 \Omega^4 \cos \Omega t + 9G^3 \Omega^4 \cos^3 \Omega t] + b_2 [-20G^5 \Omega^4 \cos^3 \Omega t + 25G^5 \Omega^4 \cos^5 \Omega t] = 0 \tag{114}$$

After simple calculation, Eq. (114) can be written

$$z_1'''' - \Omega^4 z_1 + \Theta_1 \cos \Omega t + \Theta_2 \cos 3\Omega t + \Theta_3 \cos 5\Omega t + \Theta_4 \cos 7\Omega t = 0 \tag{115}$$

where

$$\Theta_1 = -G\Omega_1 - \frac{3b_3 b_4}{4} G^3 - \frac{5b_3 b_5}{8} G^5 - \frac{35b_3 b_6}{64} G^7 - \frac{3b_1}{4} G^3 \Omega^2 - \frac{5b_2}{8} G^5 \Omega^2 - \frac{35b_6}{64} G^7 \Omega^2 + \frac{3b_1}{4} \lambda G^3 \Omega^2 + \frac{5b_2}{8} \lambda G^5 \Omega^2 + \frac{3b_1}{4} G^3 \Omega^4 + \frac{5b_2}{8} G^5 \Omega^4 \tag{116}$$

$$\Theta_2 = -\frac{b_3 b_4}{4} G^3 - \frac{5b_3 b_5}{16} G^5 - \frac{21b_3 b_6}{64} G^7 - \frac{9b_1}{4} G^3 \Omega^2 - \frac{45b_2}{16} G^5 \Omega^2 - \frac{189b_6}{64} G^7 \Omega^2 + \frac{b_1}{4} \lambda G^3 \Omega^2 + \frac{5b_2}{16} \lambda G^5 \Omega^2 + \frac{9b_1}{4} G^3 \Omega^4 + \frac{45b_2}{16} G^5 \Omega^4 \tag{117}$$

$$\Theta_3 = -\frac{b_3 b_5}{16} G^5 - \frac{7b_3 b_6}{64} G^7 - \frac{25b_2}{16} G^5 \Omega^2 - \frac{175b_6}{64} G^7 \Omega^2 + \frac{b_2}{16} \lambda G^5 \Omega^2 + \frac{25b_2}{16} G^5 \Omega^4 \tag{118}$$

$$\Theta_4 = -\frac{b_3 b_6}{64} G^7 - \frac{49b_6}{64} G^7 \Omega^2 \tag{119}$$

Requirement of no secular term needs

$$-G\Omega_1 - \frac{3b_3 b_4}{4} G^3 - \frac{5b_3 b_5}{8} G^5 - \frac{35b_3 b_6}{64} G^7 - \frac{3b_1}{4} G^3 \Omega^2 - \frac{5b_2}{8} G^5 \Omega^2 - \frac{35b_6}{64} G^7 \Omega^2 + \frac{3b_1}{4} \lambda G^3 \Omega^2 + \frac{5b_2}{8} \lambda G^5 \Omega^2 + \frac{3b_1}{4} G^3 \Omega^4 + \frac{5b_2}{8} G^5 \Omega^4 = 0 \tag{120}$$

If obtaining the first-order solution is sufficient, then Eq. (110) yields

$$\Omega_1 = \lambda^2 - \Omega^4 \tag{121}$$

Solving Ω from Eqs. (120) and (121) we have

$$\Omega = \sqrt{\frac{b_3 + \frac{3}{4} b_4 G^2 + \frac{5}{8} b_5 G^4 + \frac{35}{64} b_6 G^6}{1 + \frac{3}{4} b_1 G^2 + \frac{5}{8} b_2 G^4}} \tag{122}$$

and the corresponding approximate analytic solution is

$$z(t) = G \cos \left(\sqrt{\frac{64c_3 + 48c_4 G^2 + 40c_5 G^4 + 35c_6 G^6}{64c_0 + 48c_1 G^2 + 40c_2 G^4}} t \right) \tag{123}$$



5. Energy Balance Method

The energy balance method (EBM) [66] is another variational based method depend on the fact that at one point, the whole energy is in the form of kinetic energy while at another point, the whole energy is in the form of potential energy, and there is a balance between both forms of energies so we can take advantage from this argument. The frequency of nonlinear oscillatory problems can readily be obtained by constructing Hamiltonian and applying the collocation method. Consider the equation of nonlinear oscillator in its general form

$$z'' + f(z(t)) = 0 \tag{124}$$

The associated variational principle can be constructed as

$$V(z) = \int_0^t \left\{ -\frac{1}{2} z'^2 + F(z) \right\} dt \tag{125}$$

where $F(z) = \int f(z) dz$. The corresponding Hamiltonian is therefore can be expressed as

$$H = \frac{1}{2} z'^2 + F(z) = F(B) \tag{126}$$

followed by the consequent residual of

$$R(t) = \frac{1}{2} z'^2 + F(z) - F(B) \tag{127}$$

If we assume initial conditions as

$$z(0) = G \quad \text{and} \quad z'(0) = 0$$

Then the initial guess can be chosen as a simple harmonic motion

$$z(t) = G \cos \Omega t$$

Thus corresponding residual from Eq. (15) can be developed as

$$R(t) = \frac{1}{2} \Omega^2 G^2 \sin^2 \Omega t + F(G \cos \Omega t) - F(G) \tag{128}$$

If the initial guess is taken as the exact solution, then mathematically, we can set the value of R be zero. But the initial guess is only an approximate solution, thus R depends on t and can be set to zero. i.e,

$$\frac{1}{2} \Omega^2 G^2 \sin^2 \Omega t + F(G \cos \Omega t) - F(G) = 0$$

From [53], the residual vanishes at the specific collocation point. Therefore, collocate $\Omega t = \pi/4$ gives

$$\Omega = \lim_{\Omega t \rightarrow \pi/4} \sqrt{\frac{2F(G) - F(G \cos \Omega t)}{G^2 \sin^2 \Omega t}} \tag{129}$$

Fu et. al., [67] applied aforementioned variational based method on Eq. (15). The governing fourth-order partial differential equation is transmuted into a second-order nonlinear ordinary differential equation by employing the Galerkin method and then EBM is practiced to find the approximate analytic frequency-amplitude relationship of the nonlinear ordinary differential equation for the deflection of microbeam. The whole study is performed for doubly clamped supported boundary conditions.

6. Hamiltonian Approach

Hamiltonian approach proposed by He [68] to overcome the shortcomings of the EBM. This approach is a kind of energy method discussed previously with a vast application in conservative oscillatory systems. The terms $z'^2/2$ and $F(z)$ in Eq. (125) are the respective kinetic and potential energies of the oscillatory system expressed in Eq. (124). The corresponding Hamiltonian function can be stated as

$$H = \frac{1}{2} z'^2 + F(z) = \text{constant} = H_0 \tag{130}$$

or

$$\frac{1}{2} z'^2 + F(z) - H_0 = 0 \tag{131}$$

From Eq. (130), it is cleared that the total energy of the system remains constant during the motion (oscillation). Thus from EBM, the residual can be written by employing Eq. (127) in Eq. (131) as

$$R(t) = \frac{1}{2} \Omega^2 G^2 \sin^2 \Omega t + F(G \cos \Omega t) - H_0 \tag{132}$$



According to Eq. (130)

$$\frac{\partial H_0}{\partial G} = 0 \tag{133}$$

A new function $\tilde{H}(z)$ is introduced as

$$\tilde{H}(z) = \int_0^{T/4} \left\{ \frac{1}{2} z'^2 + F(z) \right\} dt = \frac{1}{4} TH_0 \tag{134}$$

It is cleared that

$$\frac{\partial \tilde{H}}{\partial T} = \frac{1}{4} H_0 \tag{135}$$

Then we have

$$\frac{\partial}{\partial G} \left(\frac{\partial \tilde{H}}{\partial T} \right) = 0 \tag{136}$$

or

$$\frac{\partial}{\partial G} \left(\frac{\partial \tilde{H}}{\partial (1/\Omega)} \right) = 0 \tag{137}$$

Consequently, the approximate frequency can be found from Eq. (137).

Nonlinear dynamic pull-in and pull-out analysis of viscoelastic nanoplate were studied by Shokravi [69]. Electrostatic and Casimir forces were used for actuation, and Galerkin's method was used to solve the governing equation of motion derived by Hamilton's approach. The influence of different parameters, namely, surface layer, small scale effect, coefficient of viscoelastic damping, pull-in voltage, pull-in deflection, pull-in time, and pull-out voltage, was investigated in detail.

Sedighi et al. [70] investigated the pull-in instability of nano-bridges. Hamilton's theorem and Euler's beam theory were used to finding the nanodevice's governing equation. The effect of centrifugal force, damping, Casimir, and van der Waals attractions are examined by plotting phase diagrams and time history.

7. Adomian Decomposition Method

The Adomian decomposition method (ADM) is due to George Adomian [71] and is well address in the literature. Consider the equation of motion represented with Eq. (22). The solution in this approach is illustrated with an infinite series as

$$z(t) = \sum_{n=0}^{\infty} z_n(t) \tag{138}$$

According to the basic idea of ADM, the linear operator L can be expressed as

$$L = \tilde{L} + R \tag{139}$$

where \tilde{L} is the derivative of the highest order, which is invertible, R is a linear operator of the order less than one of the order of \tilde{L} . By allowing ADM, one can write as

$$z = k - \tilde{L}^{-1}Rz - \tilde{L}^{-1}Nz \tag{140}$$

in which k denotes the terms obtained from the integration of h and then applying initial conditions. The nonlinear term and the solution can be stated as

$$Nz = \sum_{n=0}^{\infty} A_n, \quad \text{and} \quad z = \sum_{n=0}^{\infty} z_n \tag{141}$$

where A_n are called Adomian polynomial and can be formulated using the relation

$$A_n = \frac{1}{n!} \frac{d^n}{d\lambda^n} \left[H \left(\sum_{i=0}^n \lambda^i z_i \right) \right]_{\lambda=0}; \quad n = 0, 1, 2, \dots \tag{142}$$

Some of Adomian polynomial can be expressed as

$$A_1 = z_1 H'(z_0) \tag{143}$$

$$A_2 = z_2 H'(z_0) + \frac{1}{2} z_1^2 H''(z_0) \tag{144}$$

$$A_3 = z_3 H'(z_0) + z_1 z_2 H''(z_0) + \frac{1}{3} z_1^3 H'''(z_0) \tag{145}$$

$$A_4 = z_4 H'(z_0) + \left(z_1 z_3 + \frac{1}{2} z_2^2 \right) H''(z_0) + \frac{1}{2} z_1^2 z_2 H'''(z_0) + \frac{1}{24} z_1^4 H^{(iv)}(z_0) \tag{146}$$



Now comparing the like powers of x we have

$$\begin{aligned} z_0 &= k, \\ z_{n+1} &= -\tilde{L}^{-1}Rz_n - \tilde{L}^{-1}A_n, \quad n > 0 \end{aligned} \quad (147)$$

The vibration of a cantilever microbeam by a modified version of the Adomian decomposition method (ADM) was scrutinized by Duan et al. [72]. It was demonstrated that the nonlinear vdW and Casimir forces have little influence on the vibrations governed by BVP. Moreover, BVP was transformed into a nonlinear Fredholm–Volterra integral equation, and vibrational behavior was examined using modified ADM. Vibration and convergence analysis of a MEMS capacitive microphone were fully investigated by Khader and Sweilam [73]. The ADM was exerted to approximate the vibrational behavior of the model, whereas semi-group theory was utilized to prove the existence and the uniqueness of the approximate solution.

Nonlinear vibration and pull-in instability of nano-cantilever switch was thoroughly investigated by Noghrehabadi et al. [74]. Hybridization of ADM and Pade approximation was employed to solve the governing equation under intermolecular forces such as Casimir forces. It was shown that this coupling of ADM and Pade approximation gave better results than those obtained by ADM alone. The effect of different parameters on the nonlinear solution was also considered. The Timoshenko beam theory was utilized to investigate the pull-in instability and vibrations of clamped-clamped nano-switches induced by electrostatic and intermolecular forces by Moradweysi et al. [75]. Modified ADM solved the nonlinear differential equation of the objected model, and the effect of different parameters on the nonlinear behavior was also examined. The pull-in instability of carbon nanotubes-based microstructures are examined with ADM in the Refs. [76-77].

8. Miscellaneous Methods for Pull-in Instability and Periodic Behaviour of MEMS

The nonlinear dynamic behavior of nano-cantilever and clamped-clamped micro-bridge was investigated by Beni et al. [78]. Van der Waals intermolecular attractions actuated both microstructures. Euler-Bernoulli's theory of beams with the modified strain gradient theory was scrutinized for the mathematical model. The differential transform method is engaged in solving the lumped parameter model governed by nonlinear equations. The pull-in parameters of the nanosystems have been calculated as well.

The dynamic behavior of microbeam-based MEMS was examined by Rafieipour et al. [79] Euler-Bernoulli's theory was applied to find the governing equation of their objective system. The electrostatic force between microbeams was considered, and then the Galerkin procedure was utilized to obtain the differential equations of the motion of their objective system. Frequency amplitude formulation was employed to solve the equation, and the solution was expressed in closed form. The effect of various parameters on beam deflection was examined as well. The nonlinear oscillation of a MEMS oscillator was studied by Nikkar et al. [80]. Frequency amplitude formulation and Max-Min approach were utilized for finding the natural frequency of the vibration of the oscillator. It was shown that the results obtained from these two approaches are better than the results gained by EBM. A simple formula to obtain the frequency of electrically actuated microbeam is due to He et al. [81]. It was observed that only few simple calculations are needed to have highly accurate results.

9. Two-scale Mathematics

The two-scale theory is proposed by He [82] based on the fact that an absolute scale is nothing but absolute fiction. After the emergence of Einstein's theory of relativity, scientists believe in the relative observation. Implementing the relativity of scale in the same manner, one may conclude the importance of scale dependence in every scientific law. Two-scale theory proposes that the scale of observation is key factor in measurement of any object. A continuous surface may behave as discontinuous when viewed from a different perspective. Therefore, it is suggested that the scale of observation at which an object is examined or an experiment is done is the main characteristic of reference. This theory has many applications in solitary wave theory [83-84], thermoelectricity [85], microstructures [86-87], thermal science [88], nanotechnology [89] and many more [90-94].

9.1 Two-Scale MEMS

As we know, sophisticated electronic devices not only operate in the air, but can also function in various media. And if the medium is air filled with nano/micro particles, or sponges, or other porous medium, what impact will it have on their work? To solve the role of electronic devices in a porous medium, we propose a fractal MEMS model for the case of electromagnetic actuation [26-28]. At the same time, we analyze the impact on the moment of pull-in occurrence of the fractal order transformation, and get a stable pull-in condition.

Using two-scale fractal space, we can write the following relations

$$L \propto (\Delta z)^\alpha \quad (148)$$

$$z' \propto (\Delta z)^\alpha \quad (149)$$

$$z'' \propto (\Delta z)^\alpha \quad (150)$$

Because

$$\Delta t \propto \Delta z \quad (151)$$

Consequently

$$(\Delta t)^\alpha \propto (\Delta z)^\alpha \quad (152)$$

So we have

$$z'' \propto (\Delta t)^\alpha \quad (153)$$



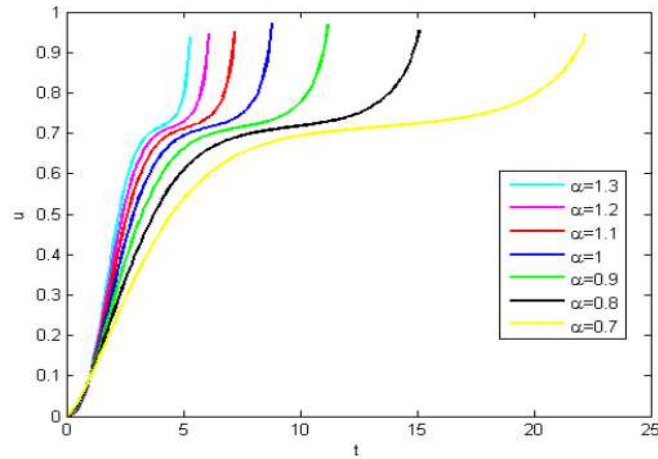


Fig. 4. Pull-in curve for various fractal dimensions

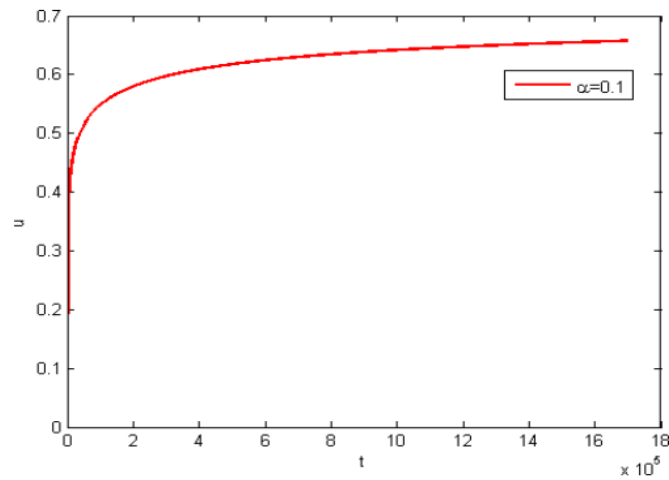


Fig. 5. Steady state of the pull-in instability

According to Eq. (153), a fractal modification of Eq. (18) is obtained

$$\frac{d^2z}{dt^{2\alpha}} + z - \frac{\kappa}{1-z} = 0 \tag{154}$$

We know that when κ does not reach the critical value, it may take the form of periodic solutions, and a pull-in phenomenon may occur when κ exceeds the critical value. As shown in Figure 4, when the value of κ is 0.20372, this figure is the pull-in curve which corresponds to different fractal dimensions. Figure 4 demonstrates that this has a huge effect on the moment when the pull-in takes place. For the two-scale dimension is greater than one, the pull-in occurs very rapidly. Later and later, the pull-in occurs with the decrease of two-scale dimension. As seen in Figure 6, the pull-in instability becomes stable for two-scale dimension is 0.1.

10. Final Remarks

The investigation of the periodic behaviour of the oscillators from microelectromechanical systems (MEMS) is the topic of this review article. Throughout numerous examples, it has examined modified asymptotic methods, for example, Laplace based variational iteration method (LVIM) and He-Laplace method. The analytical solutions provide a thorough and in-depth understanding of how system’s parameters and initial conditions affect the solution process. Analytical solutions also provide a framework for verifying and validating alternative numerical techniques.

The most notable aspect of these techniques is their high accuracy. These may also be used to solve other complex nonlinear conservative oscillatory problems. The solutions converge quickly, and their components are easy to calculate. In addition, in comparison to other analytical methods, the results need less computing work, and only one or maximum couple of iterations yield accurate results. In the last, two-scale theory and its application in MEMS in any porous medium is described briefly. Consequently, this review focused on the effective implementation of the aforementioned methods for the complex nonlinear oscillatory behaviour of MEMS problems. All of the approaches discussed in this review may be used to solve a variety of weak and strong nonlinear issues, and the worked examples used in this study can be used as paradigms for oscillatory systems.

Author Contributions

All authors contribute equally in preparation of this manuscript. All authors discussed the results, reviewed, and approved the final version of the manuscript.



Acknowledgements

This paper was supported by Natural Science Foundation of Shaanxi Province (No. 2021JQ-492).

Conflict of Interest

The authors declared no potential conflicts of interest with respect to the research, authorship, and publication of this article.

Funding

The authors received no financial support for the research, authorship, and publication of this article.

Data Availability Statements

Not applicable.

References

- [1] Gorecki, C., Bargiel, S., MEMS Scanning Mirrors for Optical Coherence Tomography, *Photonics*, 8(1), 2021, 6.
- [2] El-Hassani, N.E.A., Baraket, A., Boudjaoui, S., et al. Development and application of a novel electrochemical immune sensor for tetracycline screening in honey using a fully integrated electrochemical BioMEM, *Biosensors and Bioelectronics*, 130, 2019, 330-337.
- [3] Ghanbari, M., Rezazadeh, G., A MEMS-based methodology for measurement of effective density and viscosity of nanofluids, *European Journal of Mechanics - B/Fluids*, 86, 2021, 67-77.
- [4] Kaczynski, J., Ranacher, C., Fleury, C., Computationally efficient model for viscous damping in perforated MEMS structures, *Sensors and Actuators A: Physical*, 314, 2020, 112201.
- [5] Luo, S., Lewis, F.L., Song, Y., Ouakad, H.M., Accelerated adaptive fuzzy optimal control of three coupled fractional-order chaotic electromechanical transducers, *IEEE Transactions on Fuzzy Systems*, 29(7), 2020, 1701-1714.
- [6] Preeti, M., Guha, K., Baishnab, K.L., Sastry, A.S., Design and Analysis of a Capacitive MEMS Accelerometer as a Wearable Sensor in Identifying Low-Frequency Vibration Profiles. In: Dutta G, Biswas A, Chakrabarti A, (eds) *Modern Techniques in Biosensors. Studies in Systems, Decision and Control*, Springer, Singapore, 327, 2021.
- [7] Nuñez, D., Perdomo, O., Rivera, A., On the stability of periodic solutions with defined sign in MEMS via lower and upper solutions, *Nonlinear Analysis: Real World Applications*, 46, 2019, 195-218
- [8] He, J.H., Nurakhmetov, D., Skrzypacz, P., Wei, D., Dynamic Pull-in for Micro-Electro-Mechanical Device with a Current-Carrying Conductor, *Journal of Low Frequency Noise Vibration and Active Control*, 2019, DOI: 10.1177/1461348419847298.
- [9] Faedo, N., Dores Piuma, F.J., Giorgi, G. et al. Nonlinear model reduction for wave energy systems: a moment-matching-based approach, *Nonlinear Dynamics*, 102, 2020, 1215-1237.
- [10] Younis, M.I., *MEMS Linear and Nonlinear Statics and Dynamics*, Springer, 2011.
- [11] Lobontiu, N., *Dynamics of Microelectromechanical Systems*, Springer, 2007.
- [12] Esmailzadeh, E., Younesian, D., Askari, H., *Analytical Methods in Nonlinear Oscillations: Approaches and Applications*, Springer, 2019.
- [13] Koochi, A., Abadyan, M., *Nonlinear Differential Equations in Micro/Nano Mechanics: Application in Micro/Nano Structures and Electromechanical Systems*, Elsevier, 2020.
- [14] Zhang, W.M., Yan, H., Peng, Z.K., Meng, G., Electrostatic pull-in instability in mems/nems: a review, *Sensors and Actuators A-Physical*, 214, 2014, 187-218.
- [15] Zang, X., Zhou, Q., Chang, J., Liu, Y., Lin, L., Graphene and carbon nanotube (CNT) in MEMS/NEMS applications, *Microelectronics Engineering*, 132, 2015, 192-206.
- [16] Shariati, A., Sedighi, H.M., Żur, K.K., Habibi, M., Safa, M., On the vibrations and stability of moving viscoelastic axially functionally graded nanobeams, *Materials*, 13(7), 2020, 1707.
- [17] Tian, X., Sheng, W., Tian, F., Lu, Y., Wang, L., Simulation study on squeeze film air damping, *Micro & Nano Letters*, 15(9), 2020, 576-581.
- [18] Ouakad, H.M., Nayfeh, A.H., Choura, S., Najjar, F., Nonlinear feedback controller of a microbeam resonator, *Journal of Vibration and Control*, 21(9), 2015, 1680-1697.
- [19] Ouakad, H.M., El-Borgi, S., Mousavi, S.M., Friswell, M.I., Static and dynamic response of CNT nanobeam using nonlocal strain and velocity gradient theory, *Applied Mathematical Modelling*, 62, 2018, 207-222.
- [20] Sedighi, H.M., Size-dependent dynamic pull-in instability of vibrating electrically actuated microbeams based on the strain gradient elasticity theory, *Acta Astronautica*, 95, 2014, 111-23.
- [21] Skrzypacz, P., He, J.H., Ellis, G., Kuanysbay, M., A simple approximation of periodic solutions to microelectromechanical system model of oscillating parallel plate capacitor, *Mathematical Methods in the Applied Sciences*, 2020, <https://doi.org/10.1002/mma.6898>.
- [22] Far, M.F., Martin, F., Belahcen, A., Rasilo, P., Awan, H.A.A., Real-time control of an IPMSM using model order reduction, *IEEE Transactions on Industrial Electronics*, 68(3), 2020, 2005-2014.
- [23] Zamanzadeh, M., Ouakad, H.M., Azizi, S., Theoretical and experimental investigations of the primary and parametric resonances in repulsive force based MEMS actuators, *Sensors and Actuators A: Physical*, 303, 2020, 111635.
- [24] Moory-Shirbani, M., Sedighi, H.M., Ouakad, H.M., Najjar, F., Experimental and mathematical analysis of a piezoelectrically actuated multilayered imperfect microbeam subjected to applied electric potential, *Composite Structures*, 184, 2018, 950-960.
- [25] Zhou, S.A., On forces in microelectromechanical systems, *International Journal of Engineering Science*, 41, 2003, 313-335
- [26] Zamanzadeh, M., Jafarsadeghi-Pournaki, I., Ouakad, H.M., A resonant pressure MEMS sensor based on levitation force excitation detection, *Nonlinear Dynamics*, 100(2), 2020, 1105-1123.
- [27] Sedighi, H.M., Ouakad, H.M., Dimitri, R., Tornabene R., Stress-driven nonlocal elasticity for the instability analysis of fluid-conveying C-BN hybrid-nanotube in a magneto-thermal environment, *Physica Scripta*, 95(6), 2020, 065204.
- [28] Sedighi, H.M., Divergence and flutter instability of magneto-thermo-elastic C-BN hetero-nanotubes conveying fluid, *Acta Mechanica Sinica*, 36(2), 2020, 381-396.
- [29] He, J.H., Variational iteration method—a kind of non-linear analytical technique: some examples, *International Journal of Nonlinear Mechanics*, 34, 1999, 699-708.
- [30] Koochi, A., Farrokhhabadi, A., Abadyan, M., Modeling the size dependent instability of NEMS sensor/actuator made of nano-wire with circular cross-section, *Microsystem Technologies*, 21, 2015, 355-364.
- [31] Mohammadiana, M., Application of the variational iteration method to nonlinear vibrations of nanobeams induced by the van der Waals force under different boundary conditions, *European Physics Journal Plus*, 132, 2017, 169-181.
- [32] Farrokhhabadi, A., Mokhtari, J., Koochi, A. et al., A theoretical model for investigating the effect of vacuum fluctuations on the electromechanical stability of nanotweezers, *Indian Journal of Physics*, 89, 2015, 599-609.
- [33] Anjum, N., He, J.H., Laplace transform: making the variational iteration method easier, *Applied Mathematics Letters*, 92, 2019, 134-138.
- [34] Rastegar, S., et al., Application of He's variational iteration method to the estimation of diaphragm deflection in MEMS capacitive microphone, *Measurement*, 44, 2011, 113-120.
- [35] Anjum, N., Suleman, M., Lu, D., He, J.H., Ramzan M., Numerical iteration for nonlinear oscillators by Elzaki transform, *Journal of Low Frequency Noise Vibration and Active Control*, 39(4), 2019, 879-884.



- [36] Zhang, Y., Pang, J., Laplace-based variational iteration method for nonlinear oscillators in microelectromechanical system, *Mathematical Methods in Applied Sciences*, 2020, DOI: 10.1002/mma.6883.
- [37] He, J.H., Latifizadeh, H., A general numerical algorithm for nonlinear differential equations by the variational iteration method, *International Journal of Numerical Methods for Heat & Fluid Flow*, 30(11), 2020, 4797-4810.
- [38] Khuri, S.A., Sayfy, A., Generalizing the variational iteration method for BVPs: Proper setting of the correction functional, *Applied Mathematics Letters*, 68, 2017, 68-75.
- [39] Anjum, N., He, J.H., Analysis of nonlinear vibration of nano/microelectromechanical system switch induced by electromagnetic force under zero initial conditions, *Alexandria Engineering Journal*, 2020. <https://doi.org/10.1016/j.aej.2020.07.039>.
- [40] He, J.H., New interpretation of homotopy perturbation method, *International Journal of Modern Physics*, 20, 2006, 2561-2568.
- [41] Sedighi, H.M., Changizian, M., Noghrehabadi, A., Dynamic pull-in instability of geometrically nonlinear actuated micro-beams based on the modified couple stress theory, *Latin American Journal of Solids and Structures*, 11, 2014, 810-825.
- [42] He, J.H., Some asymptotic methods for strongly nonlinear equations, *International Journal of Modern Physics B*, 20, 2006, 1141-1199.
- [43] Qian, Y. H., et al., The spreading residue harmonic balance method for studying the doubly clamped beam-type N/MEMS subjected to the van der Waals attraction, *Journal of Low Frequency Noise Vibration and Active Control*, 38(3-4), 2019, 1261-1271.
- [44] Anjum, N., He, J.H., Nonlinear dynamic analysis of vibratory behavior of a graphene nano/microelectromechanical system, *Mathematical Methods in the Applied Sciences*, 2020, DOI: 10.1002/mma.6699.
- [45] He, J.H., Homotopy Perturbation Technique, *Computer Methods in Applied Mechanics and Engineering*, 178, 1999, 257-262.
- [46] Sedighi, H.M., Reza, A., Zare, J., Using Parameter Expansion Method and Min-Max Approach for the Analytical Investigation of Vibrating Micro-Beams Pre-Deformed by an Electric Field, *Advances in Structural Engineering*, 16(4), 2013, 693-699.
- [47] He, J.H., A Coupling Method of a Homotopy Technique and a Perturbation Technique for Non-Linear Problems, *International Journal of Nonlinear Mechanics*, 35(1), 2000, 37-43.
- [48] Keivani, M., Koochi, A., Sedighi, H.M., Abadyan, M., Farrokhabadi, A., Shahedin, A.M., Effect of surface layer on electromechanical stability of tweezers and cantilevers fabricated from conductive cylindrical nanowires, *Surface Review and Letters*, 23(02), 2016, 1550101.
- [49] Ain, Q.T., He, J.H., Anjum, N., Ali, M., The Fractional complex transform: A novel approach to the time-fractional Schrodinger equation, *Fractals*, 28(7), 2020, 2050141.
- [50] El-Dib, Y., Stability analysis of a strongly displacement time-delayed duffing oscillator using multiple scales homotopy perturbation method, *Journal of Applied and Computational Mechanics*, 4, 2018, 260-274.
- [51] Ali, M., Anjum N., Ain, Q.T., He, J.H., Homotopy Perturbation Method for the Attachment Oscillator Arising in Nanotechnology, *Fibers and Polymers*, 2020, <https://doi.org/10.1007/s12221-021-0844-x>.
- [52] Manimegalai, K., Zephania, C.F.S., Bera, P.K., et al., Study of strongly nonlinear oscillators using the Aboodh transform and the homotopy perturbation method, *European Physics Journal Plus*, 134, 2019, 462-469.
- [53] Anjum, N., He, J.H., Two modifications of the homotopy perturbation method for nonlinear oscillators, *Journal of Applied and Computational Mechanics*, 6, 2020, 1420-1425.
- [54] Koochi, A., Goharimanesh, M., Gharib, M.R., Nonlocal electromagnetic instability of carbon nanotube-based nano-sensor, *Mathematical Methods in Applied Sciences*, 2021, 1-18, DOI: 10.1002/mma.7216.
- [55] Anjum, N., Ain, Q.T., Application of He's fractional derivative and fractional complex transform for time fractional Camassa-Holm equation, *Thermal Science*, 24(5A), 2019, 3023-3030.
- [56] Gondal, M.A., Khan, M., Homotopy Perturbation Method for Nonlinear Exponential Boundary Layer Equation using Laplace Transformation, He's Polynomials and Pade Technology, *International Journal of Nonlinear Science and Numerical Simulation*, 12, 2010, 1145-1153.
- [57] Anjum, N., He, J.H., Homotopy perturbation method for N/MEMS oscillators, *Mathematical Methods in the Applied Sciences*, 2020, DOI: 10.1002/mma.6583.
- [58] Nadeem, M., Li, F.Q., He-Laplace method for nonlinear vibration systems and nonlinear wave equations, *Journal of Low Frequency Noise Vibration and Active Control*, 38(3-4), 2019, 1060-1074.
- [59] He, K., Nadeem, M., Habib, S., Sedighi, H.M., Huang, D., Analytical approach for the temperature distribution in the casting-mould heterogeneous system, *International Journal of Numerical Methods for Heat & Fluid Flow*, 2021, DOI: 10.1108/HFF-03-2021-0180.
- [60] Suleman, M., Lu, D., Yue, C., Rahman J-UL, Anjum, N., He-Laplace method for general nonlinear periodic solitary solution of vibration equations, *Journal of Low Frequency Noise Vibration and Active Control*, 38(3-4), 2018, 1297-1304.
- [61] Ghorbani, A., Beyond Adomian polynomials: He polynomials, *Chaos Solitons and Fractals*, 39, 2009, 1486-1492.
- [62] Filobello-Nino, U., Vazquez-Leal, H., Jimenez-Fernandez, V.M., et al., Enhanced classical perturbation method, *Nonlinear Science Letters A*, 9, 2018, 172-185.
- [63] Anjum, N., He, J.H., Higher-order homotopy perturbation method for conservative nonlinear oscillators generally and microelectromechanical systems' oscillators particularly, *International Journal of Modern Physics B*, 34(32), 2020, 2050313.
- [64] Ji, Q.-P., et al., Li-He's modified homotopy perturbation method coupled with the energy method for the dropping shock response of a tangent nonlinear packaging system, *Journal of Low Frequency Noise Vibration and Active Control*, 2020, DOI: 10.1177/1461348420914457.
- [65] Anjum, N., He, J.H., Ain, Q.T., Tian, D., Li-He's modified homotopy perturbation method for doubly-clamped electrically actuated microbeams-based microelectromechanical system, *Facta Universitatis, Series: Mechanical Engineering*, 2021, DOI: 10.22190/FUME210112025A.
- [66] Koochi, A., Goharimanesh, M., Nonlinear oscillations of CNT nano-resonator based on nonlocal elasticity: The energy balance method, *Reports in Mechanical Engineering*, 2(1), 2021, 41-50.
- [67] Fu, Y., Zhang, J., Wan, L., Application of the energy balance method to a nonlinear oscillator arising in the microelectromechanical system (MEMS), *Current Applied Physics*, 11, 2011, 1482-1485.
- [68] He, J.H., Hamiltonian approach to nonlinear oscillators, *Physics Letters A*, 374 (23), 2010, 2312-2314.
- [69] Shokravi, M., Dynamic pull-in and pull-out analysis of viscoelastic nanoplates under electrostatic and Casimir forces via sinusoidal shear deformation theory, *Microelectronics Reliability*, 71, 2017, 21-28.
- [70] Sedighi, H.M., Koochi, A., Abadyan, M., Nonlinear Dynamic Instability of a Double-Sided Nano-Bridge Considering Centrifugal force and Rarefied Gas Flow, *International Journal of Non-Linear Mechanics*, 77, 2015, 96-106.
- [71] Adomian, G., *Solving Frontier Problems of Physics: The Decomposition Method*, Kluwer, Boston, 1994.
- [72] Duan, J.S., et al., Solution of the model of beam-type micro- and nano-scale electrostatic actuators by a new modified Adomian decomposition method for nonlinear boundary value problems, *International Journal of Non-Linear Mechanics*, 49, 2013, 159-169.
- [73] Khader, M.M., Sweilam, N.H., Singularly perturbed BVP to estimation of diaphragm deflection in MEMS capacitive microphone: An application of ADM, *Applied Mathematics and Computation*, 281, 2016, 214-222.
- [74] Noghrehabadi, A., et al., A new approach to the electrostatic pull-in instability of nanocantilever actuators using the ADM-Padé technique, *Computers and Mathematics with Applications*, 64, 2012, 2806-2815.
- [75] Moradweysi, P., et al., Application of modified Adomian decomposition method to pull-in instability of nano-switches using nonlocal Timoshenko beam theory, *Applied Mathematical Modelling*, 54, 2018, 594-604.
- [76] Farrokhabadi, A., Koochi, A., Abadyan, M., Modeling the instability of CNT tweezers using a continuum model, *Microsystem Technologies*, 20, 2014, 291-302.
- [77] Koochi, A., Fazli, N., Rach, R., Modeling the pull-in instability of the CNT-based probe/actuator under the Coulomb force and the van der Waals attraction, *Latin American Journal of Solids and Structures*, 11, 2014, 1315-1328.
- [78] Tadi-Beni, Y., Karimpour, I., Abadyan, M., Modeling the instability of electrostatic nano-bridges and nano-cantilevers using modified strain gradient theory, *Applied Mathematical Modeling*, 39(9), 2015, 2633-2648.
- [79] Rafieipour, H., et al., Analytical approximate solution for nonlinear vibration of microelectromechanical system using he's frequency amplitude formulation, *Iranian Journal of Science and Technology Transaction B- Engineering*, 37, 2013, 83-90.
- [80] Nikkar, A., et al., Periodic solution to a nonlinear oscillator arising in micro electro mechanical system, *Journal of Vibroengineering*, 17, 2015, 2710-2717.
- [81] He, J.H., Anjum, N., Skrzypacz, P., A Variational Principle for a Nonlinear Oscillator Arising in the Microelectromechanical System, *Journal of Applied and Computational Mechanics*, 7(1), 2021, 78-83.



[82] Ain, Q.T., He, J.H., On two-scale dimension and its applications, *Thermal Science*, 23, 2019, 1707-1712.
 [83] He, J.H., Na, Q., He, C.H., Solitary waves travelling along an unsmooth boundary, *Results in Physics*, 24, 2021, 104104.
 [84] Anjum, N., Ain, Q.T., Li, X.X., Two-scale mathematical model for tsunami wave, *GEM-International Journal on Geomathematics*, 12(1), 2021, DOI: 10.1007/s13137-021-00177-z.
 [85] Liu, X.Y., Liu, Y.P., Wu, Z.W., Optimization of a fractal electrode-level charge transport model, *Thermal Science*, 25, 2021, 2213-2220.
 [86] Tian, D., Ain, Q.T., Anjum, N., Fractal N/MEMS: From pull-in instability to pull-in stability, *Fractals*, 29(2), 2020, 2150030.
 [87] Tian, D., He, C.H., A fractal micro-electromechanical system and its pull-in stability, *Journal of Low Frequency Noise Vibration and Active Control*, 2021, DOI: 10.1177/1461348420984041.
 [88] Ain, Q.T., Anjum, N., He, C.H., An analysis of time-fractional heat transfer problem using two-scale approach, *GEM-International Journal on Geomathematics*, 202, 2021, DOI: 10.1007/s13137-021-00187-x.
 [89] He, J.H., On the height of Taylor cone in electrospinning, *Results in Physics*, 17, 2020, 103096.
 [90] He, J.H., He, C.H., Sedighi, H.M., Evans model for dynamic economics revised, *AIMS Mathematics*, 6(9), 2021, 9194-9206.
 [91] Wang, K.J., A new fractional nonlinear singular heat conduction model for the human head considering the effect of febrifuge, *European Physical Journal Plus*, 135, 2020, DOI: 10.1140/epjp/s13360-020-00891-x.
 [92] Anjum, N., He, C.H., He, J.H., Two-scale fractal theory for the population dynamics, *Fractals*, 2021, DOI: 10.1142/S0218348X21501826.
 [93] Ain, Q.T., Anjum, N., Din, A., Zeb, A., Djilali, S., Khan, Z.A., On the analysis of Caputo fractional order dynamics of Middle East Lungs Coronavirus (MERS-CoV) model, *Alexandria Engineering Journal*, 61(7), 2022, 5123-5131.
 [94] Tian, D., He, C.H., He, J.H., Fractal Pull-in Stability Theory for Microelectromechanical Systems, *Frontier in Physics*, 9, 2021, 145.

Appendix A

The defined parameters in Eq. (12) are as follows

$$h_0 = \int_0^1 \xi^2 d\eta, \quad h_1 = -3 \int_0^1 \xi^3 d\eta, \quad h_2 = 3 \int_0^1 \xi^4 d\eta, \tag{A1}$$

$$h_3 = -\int_0^1 \xi^5 d\eta, \quad h_4 = -\lambda \int_0^1 \xi d\eta, \quad h_5 = \int_0^1 (\xi \xi'''' - N \xi \xi'') d\eta, \tag{A2}$$

$$h_6 = \int_0^1 (-3 \xi^2 \xi'''' + 3 N \xi^2 \xi'') d\eta, \quad h_7 = \int_0^1 (3 \xi^3 \xi'''' - 3 N \xi^3 \xi'') d\eta - \alpha \int_0^1 \xi \xi'' d\eta \int_0^1 \xi'^2 d\eta, \tag{A3}$$

$$h_8 = \int_0^1 (-\xi^4 \xi'''' + N \xi^4 \xi'') d\eta + 3 \alpha \int_0^1 \xi^2 \xi'' d\eta \int_0^1 \xi'^2 d\eta, \quad h_9 = -3 \alpha \int_0^1 \xi^3 \xi'' d\eta \int_0^1 \xi'^2 d\eta, \tag{A4}$$

$$h_{10} = \alpha \int_0^1 \xi^4 \xi'' d\eta \int_0^1 \xi'^2 d\eta \tag{A5}$$

Appendix B

The defined parameters in Eq. (12) are as follows

$$c_0 = \int_0^1 \xi^2 d\eta, \quad c_1 = -2 \int_0^1 \xi^4 d\eta, \quad c_2 = \int_0^1 \xi^6 d\eta, \quad c_3 = \int_0^1 (\xi \xi'''' - \sigma \xi \xi'' - \mu^2 \xi^2) d\eta, \tag{B1}$$

$$c_4 = \int_0^1 \left(-2 \xi^3 \xi'''' + 2 \sigma \xi^3 \xi'' - \beta \xi \xi'' \int_0^1 \xi'^2 d\eta \right) d\eta, \quad c_5 = \int_0^1 \left(\xi^5 \xi'''' - \sigma \xi^5 \xi'' + 2 \beta \xi^3 \xi'' \int_0^1 \xi'^2 d\eta \right) d\eta, \tag{B2}$$

$$c_6 = -\int_0^1 \left(\beta \xi^5 \xi'' \int_0^1 \xi'^2 d\eta \right) d\eta \tag{B3}$$

where the parameters σ , β and μ are nondimensional and are as follows

$$\sigma = \frac{\tilde{N}L^2}{EI}, \quad \beta = 6 \left(\frac{d}{h} \right)^2, \quad \mu = \frac{24L^4 \nu^2 \epsilon_v}{Ed^3 h^3} \tag{B4}$$

Appendix C

The coefficient of Eq. (24) are as follows

$$\Theta_0 = -G\Omega^2 \left(\frac{d_1 G}{2} + \frac{3d_3 G^3}{8} \right) + d_4 + \frac{d_6 G^2}{2} + \frac{3d_8 G^4}{8} + \frac{5d_{10} G^6}{16} \tag{C1}$$


$$\Theta_1 = -G\Omega^2 \left(1 + \frac{3d_2 G^2}{4} \right) + Gd_5 + \frac{3d_7 G^3}{4} + \frac{5d_9 G^5}{8}, \quad \Theta_2 = -G\Omega^2 \left(\frac{d_1 G}{2} + \frac{d_3 G^3}{2} \right) + \frac{d_6 G^2}{2} + \frac{d_8 G^4}{2} + \frac{15d_{10} G^6}{32} \tag{C2}$$





$$\Theta_3 = -G\Omega^2 \left(\frac{d_2 G^2}{4} \right) + \frac{d_7 G^3}{4} + \frac{5d_9 G^5}{16}, \quad \Theta_4 = -G\Omega^2 \left(\frac{d_3 G^3}{8} \right) + \frac{d_8 G^4}{8} + \frac{3d_{10} G^6}{16} \quad (C3)$$


$$\Theta_5 = \frac{d_9 G^5}{16}, \quad \text{and} \quad \Theta_6 = \frac{d_{10} G^6}{32} \quad (C4)$$

ORCID iD

Naveed Anjum  <https://orcid.org/0000-0001-7810-7877>

Ji-Huan He  <https://orcid.org/0000-0002-1636-0559>

Chun-Hui He  <https://orcid.org/0000-0003-0810-5248>

Alina Ashiq  <https://orcid.org/0000-0002-3502-5932>



© 2022 Shahid Chamran University of Ahvaz, Ahvaz, Iran. This article is an open access article distributed under the terms and conditions of the Creative Commons Attribution-NonCommercial 4.0 International (CC BY-NC 4.0 license) (<http://creativecommons.org/licenses/by-nc/4.0/>).

How to cite this article: Anjum N., He J.H., He C.H., Ashiq A. A Brief Review on the Asymptotic Methods for the Periodic Behaviour of Microelectromechanical Systems, *J. Appl. Comput. Mech.*, 8(3), 2022, 1120–1140.
<https://doi.org/10.22055/jacm.2022.39404.3401>

Publisher's Note Shahid Chamran University of Ahvaz remains neutral with regard to jurisdictional claims in published maps and institutional affiliations.

